JACS
JOURNAL OF THE AMERICAN CHEMICAL SOCIETY
Article
pubs.acs.org/JACS

P–N/P–P Bond Metathesis for the Synthesis of Complex Polyphosphanes

Kai-Oliver Feldmann[†,‡] and Jan J. Weigand*[,†]

[†]Institut für Anorganische und Analytische Chemie and [‡]Graduate School of Chemistry, Westfälische Wilhelms-Universität Münster, Corrensstrasse 30, 48149 Münster, Germany

Supporting Information

ABSTRACT: A unique hexaphosphane featuring a 2,2′-bi(1,2,3-triphosphacyclopentane) moiety (**19**) and an ethylene-bridged bis-isotetraphosphane (**27**^{c,m}) were both selectively prepared in efficient one-pot syntheses from easily accessible tris(3,5-dimethyl-1-pyrazolyl)phosphane (**14**) and 1,2-bis(phenylphosphanyl)ethane (**18**^{c,m}). The formation of **27**^{c,m} is an example of a highly efficient P–P bond formation via protolysis. In contrast, the formation of **19** comprises P–N/P–P bond metathesis steps. This constitutes a novel synthetic approach toward the preparation of complex polyphosphanes. Detailed spectroscopic investigations form the basis for a mechanistic understanding of this unprecedented methodology. Furthermore, the preparation of a unique dinuclear iron–carbonyl complex which features hexaphosphane **19** as a bridging ligand illustrates the potential use of complex polyphosphanes such as **19** as ligands in transition metal chemistry.

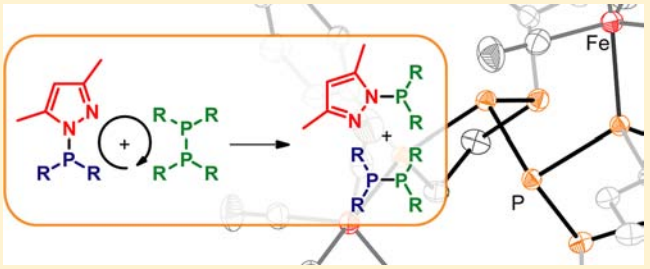

INTRODUCTION

Polyphosphanes display a fascinating structural variety which illustrates the propensity of phosphorus to form P–P bonds in a multitude of acyclic, cyclic, and cagelike motifs.[1−4] Several synthetic methods for the preparation of polyphosphanes from P_1-sources were developed[4,5] and certainly form the basis for the structural diversity within this class of compounds. Scheme 1 summarizes the most important synthetic methods for the generation of P–P bonds. Salt metathesis reactions of a metal phosphide with a halophosphane are most commonly employed (Scheme 1, method A).[4] The required phosphides are usually accessed via in situ reduction of a halophosphane with a group 1 or 2 metal (method A1)[4] or the reaction of silyl-substituted phosphanes with lithium alkyls (method A2).[5a] Silyl- or stannyl-substituted phosphanes may be alternatively reacted with chlorophosphanes.[5b] The driving force for this P–P coupling reaction is the formation of the strong Si–Cl (490 ± 3 kJ mol^{-1}) or Sn–Cl (425 ± 17 kJ mol^{-1}) bonds, respectively (Scheme 1, method B).[6] In the presence of a base, coupling of a halophosphane and a primary or secondary phosphane can be effected (method C). This procedure is typically used for the preparation of cyclophosphanes with thermodynamically favored ring sizes.[7] Similarly, reactions of secondary phosphanes and amino-substituted phosphanes[8] yield P–P bonded compounds with concomitant formation of a secondary amine (method D). These reactions commonly require elevated temperatures. Some transition metal-[1,9] and main group-mediated approaches[10] are described as well. For example, P–P bond formation can be achieved via catalytic dehydrogenative coupling of primary and secondary phosphanes using, for example, Ru-based catalysts (method E).[11]

Scheme 1. Selected Synthetic Methods A–E for the Generation of P–P Bonds in Polyphosphanes

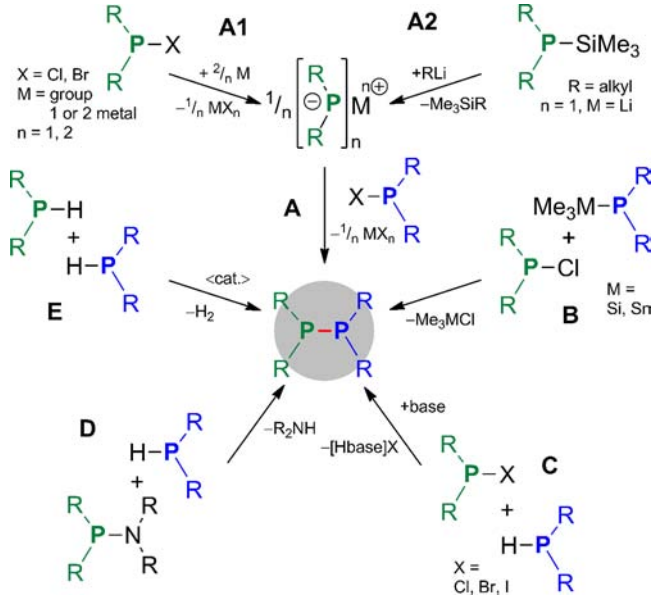

Despite these many different methods for P–P bond formation, the preparation of complex polyphosphanes is commonly either a nonselective low yielding process requiring laborious workup procedures or a tedious multistep procedure.

Received: June 10, 2012
Published: September 10, 2012

dx.doi.org/10.1021/ja305406x | J. Am. Chem. Soc. 2012, 134, 15443−15456

Harsh conditions, such as elevated temperatures, highly basic media, and use of demanding and very toxic reagents are often necessary. For example, the preparation of hexaphosphane **2a** (Scheme 2; **a**: R = *i*Pr, **b**: R = *t*Bu) requires as many as six steps,

Scheme 2. Exemplary Preparation of Lithium Triphosphide Li[1a] and Synthesis of Hexaphosphanes 2a,b (a: R = *i*Pr, b: R = *t*Bu)

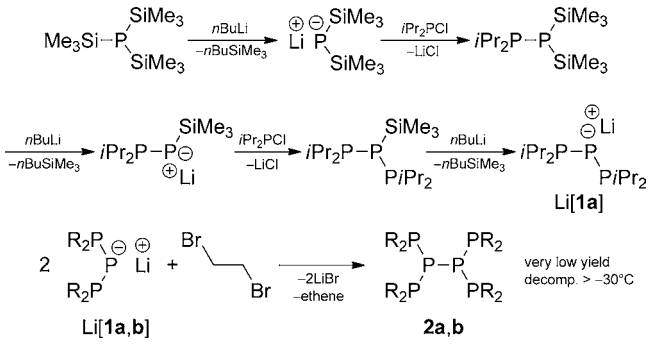

starting from $P(SiMe_3)_3$ as the P_1 unit.[12] The last step involves reductive coupling of 2 equiv of triphosphide Li[**1a**] with 1,2-dibromoethane, yielding a complex product mixture. Hexaphosphane **2a** cannot be isolated and readily decomposes in the reaction mixture above −30 °C. Nevertheless, it is structurally characterized.[12] The same holds true for the *t*Bu-substituted derivative **2b**,[13] even though a more efficient synthesis for Li[**1b**] is available.[13a] Decomposition pathways of polyphosphanes are often discussed to proceed via disproportionation reactions accompanied by P−P bond rupture and intermolecular scrambling processes.[14,15] Very few cases of selective scrambling reactions involving di- and polyphosphanes were reported. Trifluoromethyl- (**3**)[16] or *t*Bu-substituted (**4**)[17] diphosphanes, for example, react with tetramethyldiphosphane (**5**) to quantitatively form the nonsymmetrically substituted diphosphanes **6** and **7** (Scheme 3).

Scheme 3. Two Examples of P−P/P−P Metathesis Reactions in which Symmetrically Substituted Diphosphanes 3−5 Scramble in Solution Quantitatively to the Nonsymmetrically Substituted Diphosphanes 6 and 7[a]

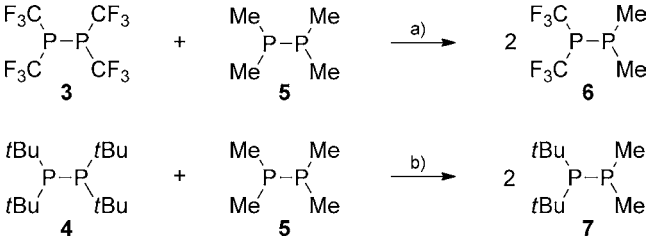

[a](a) C_6D_6, RT, reaction time not indicated; (b) CH_2Cl_2, RT, 14 days.

From a more general perspective, this reaction allows for the crosswise exchange of bonding partners of the starting materials A−B and C−D to form the products A−D and C−B. This is a typical feature of a bond metathesis as, for example, found in olefin metathesis (denoted here as C−C/C−C bond metathesis; Scheme 4, top). In these reactions, the total number of bonds remains constant.[18] Accordingly, scrambling reactions of di- and polyphosphanes can be considered as P−P/P−P bond metatheses (Scheme 4, middle).

Scheme 4. Generalized Reaction Equations of Bond Metathesis Reactions of Type C−C/C−C, P−P/P−P, and P−N/P−P

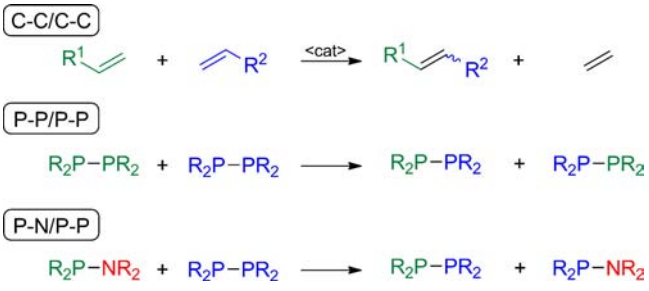

Related reactions of diphosphanes were reported with compounds comprising P−H,[16,19] P−Cl,[16] or P−N bonds. To the best of our knowledge, only one example is known for the latter. If diphosphane **3** is reacted with Me_2PNMe_2 (**8**) quantitative conversion to mixed diphosphane **9** and $(F_3C)_2PNMe_2$ (**10**) is observed (Scheme 5, eq I).[16] A related

Scheme 5. Formation of Diphosphanes 9 and 13 via P−N/P−P Exchange[a]

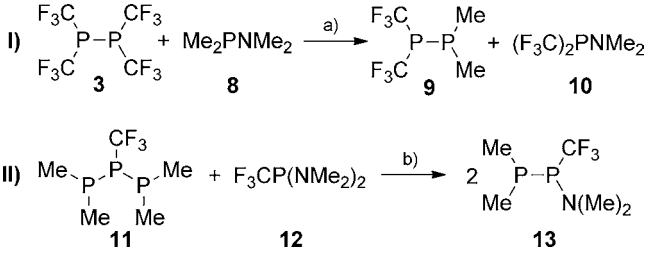

[a](a) C_6D_6, RT, quantitative in solution; (b) neat, 132 °C, 2 h.

reaction was reported for triphosphane **11** which reacts with $F_3CP(NMe_2)_2$ (**12**) to form diphosphane **13** (Scheme 5, eq II). This reaction, however, requires elevated temperatures (132 °C) and leads to a mixture of products.[17]

Additional protocols for the generation of P−P bonds are vital to further develop polyphosphane chemistry. During our investigations of the reactivity of highly charged phosphorus cations with nucleophiles,[20] we found that the P−N bonds in pyrazolyl-substituted P^{III} compounds are particularly labile and can be easily cleaved.[21] Accordingly, tri- and isotetraphosphane **15** and **16** can be prepared via the reaction of tris(3,5-dimethyl-1-pyrazolyl)phosphane (**14**, pyr = 3,5-dimethyl-1-pyrazolyl)[22] with secondary phosphane Cy_2PH in excellent yields (Scheme 6).[23] This approach toward P−P bond formation is related to the reaction of primary or secondary phosphanes with alkylaminophosphanes (Scheme 1, method D).[8] The use of pyrazolylphosphanes, however, is advantageous, as the reactions proceed at ambient temperature and the yields are excellent. In extension, we now report on the formation of polyphosphanes via unprecedented P−N/P−P bond metathesis (Scheme 4, bottom). This constitutes a novel synthetic approach and, therefore, opens a new avenue in polyphosphane chemistry.

RESULTS AND DISCUSSION

By analogy with the reaction of Cy_2PH with **14** we assumed that the related reaction of a bis-secondary phosphane, such as bis(phenylphosphanyl)ethane[24] with **14** would result in the formation of two P−P bonds, yielding a symmetrically

dx.doi.org/10.1021/ja305406x | J. Am. Chem. Soc. 2012, 134, 15443−15456

Scheme 6. Preparation of Triphosphane 15 and Isotetraphosphane 16 from 14 and Cy_2PH[a]

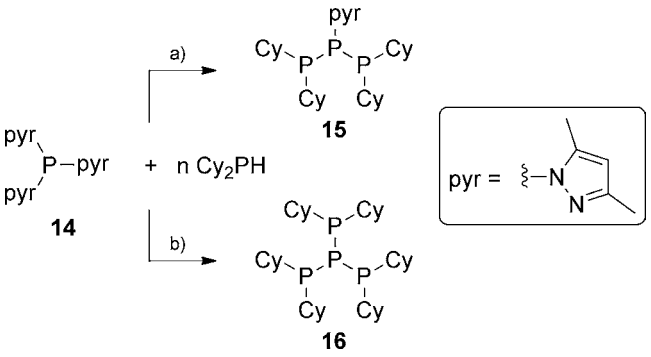

[a](a) n = 2, −2 3,5-dimethylpyrazole (**17**), CH_3CN, RT, 15 h, 91%; (b) n = 3, −3 **17**, CH_3CN, RT, 7 d, 95%; pyr =3,5-dimethyl-1-pyrazolyl.

substituted triphosphane (Scheme 7, R = Ph). This type of bond formation is a comproportionative coupling and is denoted here as type I.

Scheme 7. Generalized P–P Bond Formation via Reactions of a Bis-secondary Phosphane and 14 (3,5-dimethylpyrazole = 17)

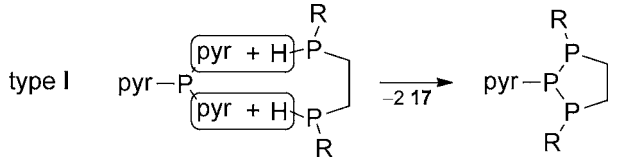

The reaction of 1,2-bis(phenylphosphanyl)ethane **18**[c,m] (~1:1 mixture of the chiral (*rac*-**18**[c]) and achiral (*meso*-**18**[m]) diastereomers; c = chiral, m = meso) and **14** in a 1:1 ratio in CH_3CN yielded a colorless precipitate which was isolated by filtration, washed several times with CH_3CN and dried in vacuo. The $^{31}P\{^1H\}$ NMR spectrum of the dissolved precipitate (CD_2Cl_2, 300 K) is depicted in Figure 1 and confirms the formation of a single, highly symmetrical product which was subsequently identified as hexaphosphane **19**. Single crystals suitable for X-ray single crystal structure determination were obtained by slow diffusion of *n*-hexane into a solution of **19** in CH_2Cl_2. The molecular structure of **19** is depicted in Figure 2. An inversion symmetrical arrangement of two 1,2,3-triphosphacyclopentane rings fused via the central phosphorus atoms in an antiperiplanar fashion is observed. The P–P bond lengths are comparable to those of the respective bonds in related hexaphosphanes **2a**,**b**[12,13c] (e.g., P2–P2i: 2.2337(7) Å vs 2.1873(9) Å in **2a** and 2.200(2) Å in **2b**). In contrast to **2a**,**b** the P1–P2–P3 angle in **19** (97.81(2)°) is defined by the five-membered ring geometry and is therefore significantly more acute than in the related acyclic derivatives (**2a**: 113.11(2)°;[12] **2b**: 107.10(4)°[13c]). The P2^i–P2–P1 (93.21(2)°) and P2^i–P2–P3 (95.56(2)°) angles in **19** are more acute than the corresponding angles in the related hexaphosphanes (**2a**: 117.98(7) and 116.10(7)°;[12] **2b**: 107.95(4) and 112.09(4)°[13c]). This is attributed to the antiperiplanar conformation with respect to the P2–P2^i bond. In contrast, hexaphosphanes **2a**[12] and **2b**[13c] display a gauche conformation resulting in increased steric repulsion and thus in larger bond angles. Similar to other structurally characterized 1,2,3-triphosphacyclopentane derivatives, a twist ($^4T_5$)[25,26] con-

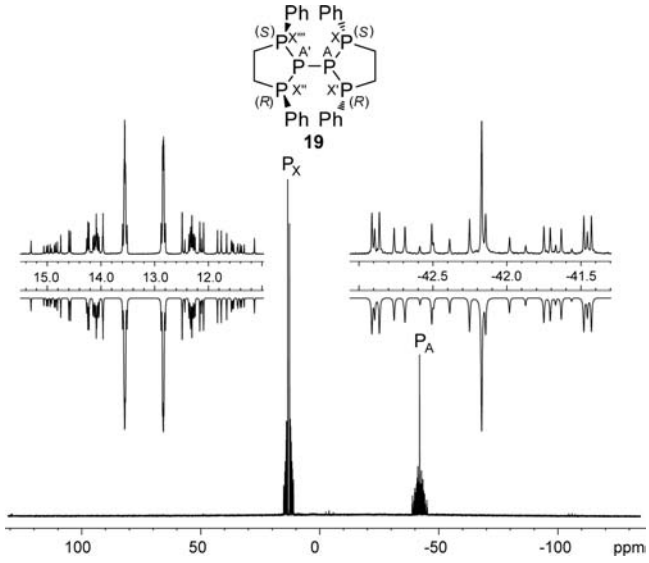

Figure 1. $^{31}P\{^1H\}$ NMR spectrum of **19** (CD_2Cl_2, 300 K; insets show experimental (upward) and fitted spectra (downward)); AA′XX′X″X‴ spin system: $\delta(P_A)$ = −41.8 ppm, $\delta(P_X)$ = 13.2 ppm; $^1J(P_AP_{A'})$ = −137.0 Hz, $^1J(P_AP_X)$ = $^1J(P_AP_{X'})$ = $^1J(P_{A'}P_{X''})$ = $^1J(P_{A'}P_{X'''})$ = −258.5 Hz, $^2J(P_AP_{X''})$ = $^2J(P_AP_{X'''})$ = $^2J(P_{A'}P_X)$ = $^2J(P_{A'}P_{X'})$ = 142.5 Hz, $^2J(P_XP_{X'})$ = $^2J(P_{X''}P_{X'''})$ = 1.9 Hz, $^3J(P_XP_{X'''})$ = $^3J(P_{X'}P_{X''})$ = 31.7 Hz, $^3J(P_XP_{X''})$ = $^3J(P_{X'}P_{X'''})$ = 49.5 Hz.

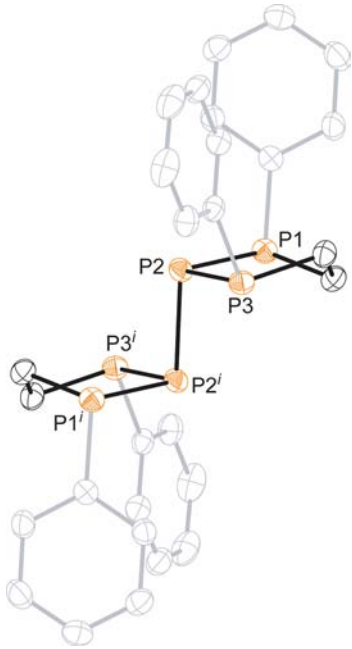

Figure 2. Molecular structure of **19** (hydrogen atoms are omitted for clarity and thermal ellipsoids are displayed at 50% probability); selected bond lengths [Å] and angles [deg]: P1–P2 2.2075(5), P2–P3 2.2270(5), P2–P2^i 2.2337(7); P1–P2–P3 97.81(2), P1–P2–P2^i 93.21(2), P3–P2–P2^i 95.56(2); i = −x+2, −y+1, −z.

formation is observed for the 1,2,3-triphosphacyclopentane rings (Figure 3**A**,**B**).[27] The substituents on this fragment adopt an all-trans arrangement (Figure 3, **A**). This is in agreement with prior reports of 1,2,3-triphosphacyclopentane derivatives which indicate that a cis–trans arrangement (Figure 3, **B** and **D**) is thermodynamically less favorable and only observed for substituents of very small steric demand.[28]

dx.doi.org/10.1021/ja305406x | J. Am. Chem. Soc. 2012, 134, 15443–15456

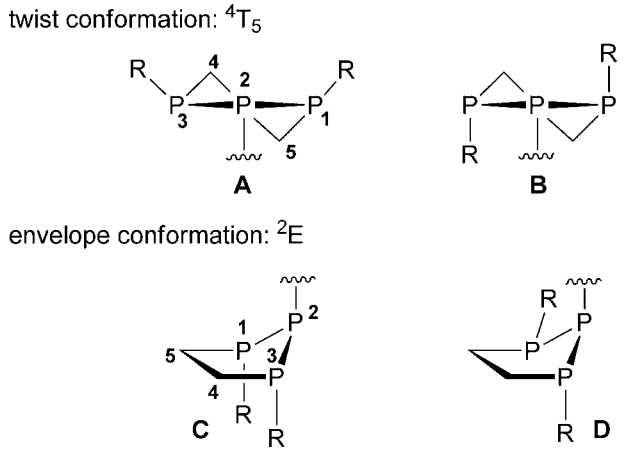

Figure 3. All-trans and cis–trans conformers of 1,2,3-substituted 1,2,3-triphosphacyclopentanes. The twist conformer ($^4T_5$, **A** and **B**) is defined by the coplanarity of three atoms and the midpoint of the opposite bond; C4 is located above, C5 below the plane. The envelope conformer (^2E, **C** and **D**) is defined by four coplanar atoms with one phosphorus atom (P2) above the plane.

The observation of an AA′XX′X″X‴ spin system in the $^{31}P\{^1H\}$ NMR spectrum of **19** is in contrast to the molecular structure in the solid state. A twist conformer as observed in the solid state would render the P1 and P3 atoms chemically unequal which would be inconsistent with the observed spin system. Therefore, it is proposed that the conformation in solution is best understood as a time-averaged envelope conformation of an *all-trans*-1,2,3-triphosphacyclopentane moiety (Figure 3, C). This is in line with previously reported spectroscopic analyses of 1,2,3-triphosphacyclopentane derivatives[28] and related interconversion processes of the conformers of organic five-membered rings.[29,30] Indication for the presence of a cis–trans isomer of **19** (Figure 3, **D**) is not observed. The chemical shift of the resonance corresponding to P_A ($\delta(P_A)$ = −41.8 ppm) is in the expected range for the central P atom of isotetraphosphanes (e.g., $(Ph_2P_M)_3P_A$ $\delta(P_A)$ = −57.2 ppm; THF).[31] The resonance corresponding to P_X in **19** ($\delta(P_X)$ = 13.2 ppm) compares well with those reported for P atoms incorporated in a saturated five-membered ring (e.g., P_B in *all-trans*-1,2,3-triphenyl-1,2,3-triphosphacyclopentane (**20**), AB_2 spin system, $\delta(P_A)$ = −14.7 ppm, $\delta(P_B)$ = 17.2 ppm, $^1J(P_AP_B)$ = 273 Hz).[32] The $^1J(P_AP_X)$ coupling constant (−258.5 Hz) derived from the fit[33] of the experimental $^{31}P\{^1H\}$ NMR spectrum is also comparable to the corresponding coupling in **20** ($^1J(P_AP_B)$ = 273 Hz). It is noteworthy that the NMR spectroscopic parameters of **19** are remarkably distinct from those reported for **2a**,**b**.[12,13a] Importantly, the absolute value of the $^1J(P_AP_{A'})$ coupling constant in **19** (137.0 Hz) is distinctly smaller than the corresponding coupling constants observed for **2a**,**b** (**a**: $^1J(P_AP_{A'})$ = 669 Hz; **b**: $^1J(P_AP_{A'})$ = 467.5 Hz). This small coupling constant is in agreement with the substantially smaller sum of the bond angles (Σ)[34] on the P_A atoms of **19** (Σ = 286.6°) compared to the corresponding parameter of compounds **2a**,**b** (**2a**: Σ = 347.2°; **2b**: Σ = 327.1°) and, furthermore, indicates a predominantly antiperiplanar arrangement of the lone pairs of electrons on P_A and $P_{A'}$ in **19** in solution.[35]

Analytically pure **19** appears to be indefinitely stable in the solid state (under Ar or N_2) at ambient temperature and has a defined melting range (197–199 °C). Compound **19** is reasonably soluble in benzene, poorly soluble in CH_2Cl_2 (~10 mg/mL), and insoluble in CH_3CN. To illustrate the stability of compound **19** and its potential use as a multidentate ligand toward transition metal moieties, complex **21** was prepared via the reaction of 2 equiv of $Fe_2(CO)_9$ with hexaphosphane **19** in THF (Scheme 8). The reaction

Scheme 8. Preparation of Complex 21 from the Reaction of 19 and $Fe_2(CO)_9$[a]

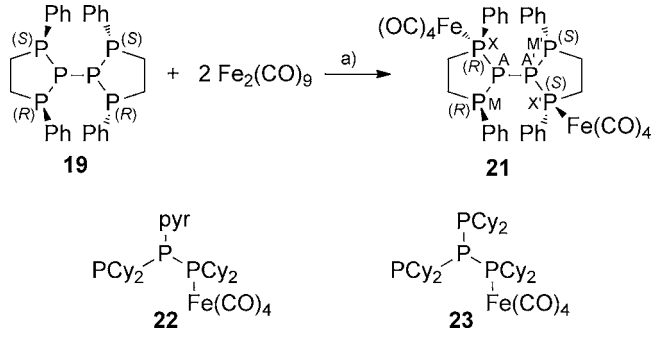

[a](a) −2 $Fe(CO)_5$, THF, RT, 72 h, 28% (top); examples for polyphosphane–$Fe(CO)_4$ complexes (**22** and **23**, bottom).[23]

proceeded smoothly at ambient temperature in the dark, and compound **21** was found to be the major product in solution after a reaction time of 72 h according to ^{31}P NMR spectroscopic investigations. Significant decomposition of the hexaphosphane framework was not observed. All volatiles were removed from the reaction mixture in vacuo, and the residue was dissolved in toluene. Slow evaporation of toluene at −18 °C yielded **21** as orange crystals in 28% yield (not optimized). The molecular structure of **21** (Figure 4) shows hexaphosphane **19** coordinated to two $[Fe(CO)_4]$ moieties. The coordinating phosphorus atoms in **21** (P1, $P1^i$) occupy an axial position of the pseudotrigonal bipyramidal coordination spheres around the iron atoms. This mode of coordination is reminiscent of that in the previously reported iron complexes **22** and **23** (Scheme 8, bottom).[23]

The coordination of the P_6-core to the iron–carbonyl moieties in **21** does not show a significant influence on the P–P bond lengths. However, the P_6 framework in **21** adopts a gauche arrangement which is in contrast to the antiperiplanar arrangement observed in the molecular structure of **19**. This change in the conformation of the P_6-core is attributed to steric effects, because an antiperiplanar arrangement would result in strong steric repulsion of the $[Fe(CO)_4]$ moieties. As a result of the gauche conformation, the P2–P3 and $P2^i$–$P3^i$ bonds are almost eclipsed (dihedral angle 19.93(3)°) which results in a widening of the P3–P2–P2′ angle in **21** (105.46(1)°) in comparison to the respective angle in **19** (95.56(2)°). The $^{31}P\{^1H\}$ NMR spectrum of **21** (CD_2Cl_2, 300 K, Figure 5) displays an AA′MM′XX′ spin system. The chemical shifts of the P_A (−47.4 ppm) and P_M (15.3 ppm) atoms are similar to those of the respective resonances of **19** ($\delta(P_A)$ = −41.8 ppm, $\delta(P_X)$ = 13.8 ppm). In contrast, the resonance of the P atoms coordinated to the iron atoms is shifted to significantly lower field ($\delta(P_x)$ = 93.0 ppm). A similar downfield shift upon coordination to $[Fe(CO)_4]$ moieties was also observed for the related complexes **22** and **23**.[23] The absolute value of the $^1J(P_AP_{A'})$ coupling constant ($^1J(P_AP_{A'})$ = −317.5 Hz) is significantly larger than the absolute value of the respective

dx.doi.org/10.1021/ja305406x | J. Am. Chem. Soc. 2012, 134, 15443–15456

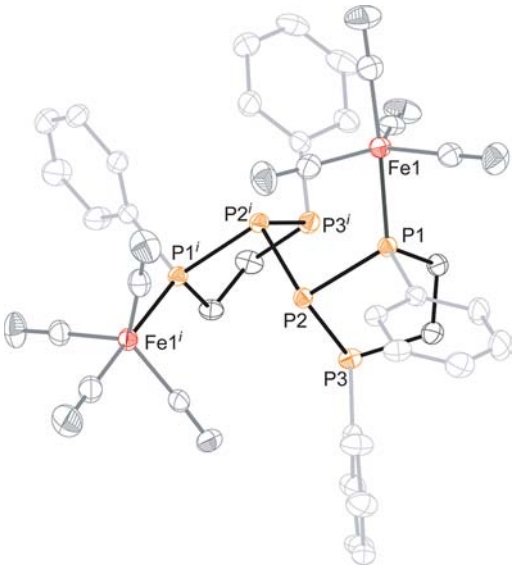

Figure 4. Molecular structure of **21** (hydrogen atoms are omitted for clarity and thermal ellipsoids are displayed at 50% probability); selected bond lengths [Å] and angles [deg]: P1–P2 2.2179(5), P1–Fe1 2.2399(4), P2–P2^i 2.2270(7), P2–P3 2.2297(5); P2–P1–Fe1 119.63(2), P1–P2–P2^i 97.71(2), P1–P2–P3 95.74(2), P2^i–P2–P3 105.46(1), C16–Fe1–C17 114.07(8), C16–Fe1–C18 117.54(8), C17–Fe1–C18 128.28(8), C16–Fe1–C15 92.69(7), C17–Fe1–C15 91.34(7), C18–Fe1–C15 89.49(8), C16–Fe1–P1 89.88(5), C17–Fe1–P1 88.74(5), C18–Fe1–P1 88.23(5), C15–Fe1–P1 177.15(6); i = $-x$, y, $-z+1/2$.

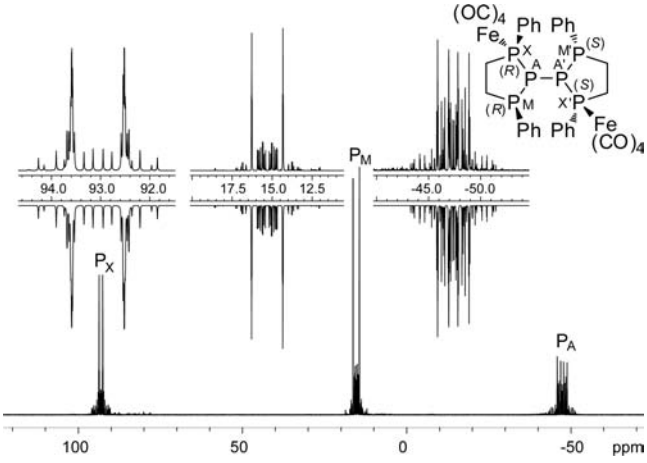

Figure 5. $^{31}P\{^1H\}$ NMR spectrum of **21** (CD_2Cl_2, 300 K; insets show experimental (upward) and fitted spectra (downward)); AA′MM′XX′ spin system: $\delta(P_A)$ = −47.4 ppm, $\delta(P_M)$ = 15.3 ppm, $\delta(P_X)$ = 93.0 ppm; $^1J(P_AP_{A'})$ = −317.5 Hz, $^1J(P_AP_M)$ = −314.0 Hz, $^1J(P_AP_X)$ = −276.7 Hz, $^2J(P_AP_{M'})$ = $^2J(P_{A'}P_M)$ = −2.0 Hz, $^2J(P_AP_{X'})$ = $^2J(P_{A'}P_X)$ = 103.1 Hz, $^2J(P_MP_X)$ = $^2J(P_{M'}P_{X'})$ = 1.1 Hz, $^3J(P_MP_{M'})$ = 163.8 Hz, $^3J(P_MP_{X'})$ = $^3J(P_{M'}P_X)$ = 5.3 Hz, $^3J(P_XP_{X'})$ = 51.0 Hz.

coupling constant in **19** ($^1J(P_AP_{A'})$ = −137.0 Hz). This is attributed to a predominantly gauche conformation with respect to the P_A–$P_{A'}$ bond in **21**. The comparably large $^3J(P_MP_{M'})$ coupling constant indicates a short distance between the lone pairs of electrons on the P_M atoms.[4b] Thus, the eclipsed arrangement of the P2–P3 and P2^i–P3^i bonds observed in the solid state apparently also constitutes the major contribution to the conformation of **21** in solution.

Furthermore, the introduction of the [Fe(CO)$_4$] moiety causes a significant increase in the absolute value of the ^1J(PP) coupling constant via the P–P bonds adjacent to P–P bonds which involve the coordinated P atom (defined as $^1J(PP)_{remote}$, Table 1). This effect is also observed for complexes **22** and

Table 1. $^1J(PP)_{remote}$ and $^1J(PP)_{close}$ Coupling Constants of Complexes 21–23 and the Corresponding Free Ligands 15, 16, and 19

	$^1J(PP)_{remote}$ [Hz]	$^1J(PP)_{close}$ [Hz]
	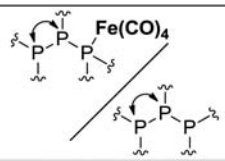	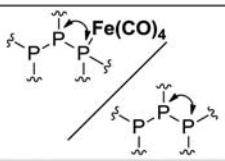
22[23]	−382	−326
15[23]	−272	−272
23[23]	−465	−345
16[23]	−362	−362
21	−318, $^1J(P_AP_{A'})$ −314, $^1J(P_AP_M)$	−277
19	−137, $^1J(P_AP_{A'})$ −259, $^1J(P_AP_X)$	−259

23.[23] The respective values of the iron complexes (gray rows) along with the corresponding coupling constants of the free ligands (white rows) are listed in Table 1. In contrast, the absolute values of the ^1J(PP) coupling constants involving the coordinated P atom ($^1J(PP)_{close}$) are not uniformly larger than the absolute values of the corresponding coupling constants in the free ligands (Table 1).

Overall, compound **19** represents the first isolable and fully characterized hexaphosphane featuring this bonding motif and the corresponding iron–carbonyl complex **21** is unprecedented. Nevertheless, the formation of hexaphosphane **19** raises several questions because we initially assumed that the reaction of **14** and **18**^{c,m} would proceed according to the previously introduced reaction pathway type I (Scheme 7, R = Ph). Consequently, the formation of *all-trans*-triphosphane **24** and pyrH (**17**) was anticipated (Scheme 9). This is apparently not the case, rendering further investigations necessary to gain a detailed understanding of the reaction.

The $^{31}P\{^1H\}$ NMR spectrum of the supernatant solution of the reaction of **18**^{c,m} and **14** in a 1:1 ratio is depicted in Figure 6. Resonances corresponding to a series of different compounds

Scheme 9. Anticipated Formation of Compound 24 from the Reaction of 18^{c,m} and 14 in a Ratio of 1:1[a]

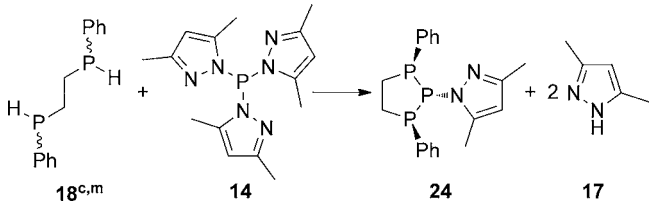

18^{c,m} **14** **24** **17**

[a]The reaction with **18**^{m} is preferred (see text).

dx.doi.org/10.1021/ja305406x | J. Am. Chem. Soc. 2012, 134, 15443–15456

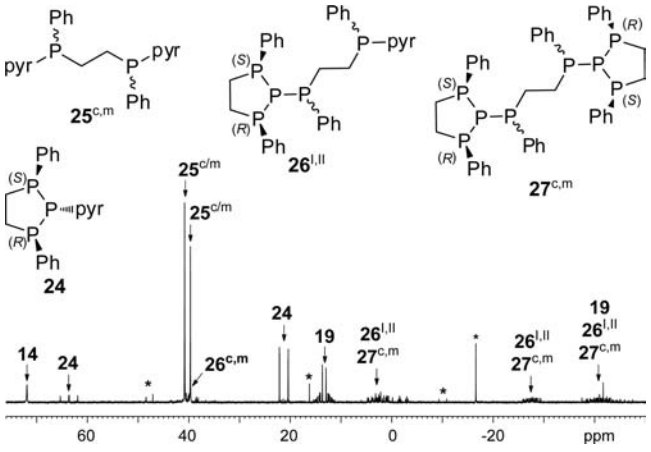

Figure 6. $^{31}P\{^{1}H\}$ NMR spectrum of the supernatant of the reaction of **14** and **18**^{c,m} in a 1:1 ratio (CH_2Cl_2, C_6D_6 capillary, 300 K).

are observed. Residual phosphane **14** (δ = 72.4 ppm)[22] and hexaphosphane **19** are identified next to small amounts of triphosphane **24**. We were able to isolate a very small amount (8.0 mg) of the oxygen- and moisture-sensitive triphosphane **24** from the reaction mixture by column chromatography which allowed for spectroscopic characterization. The $^{31}P\{^{1}H\}$ NMR spectrum is depicted in Figure 7. Resonances of a characteristic

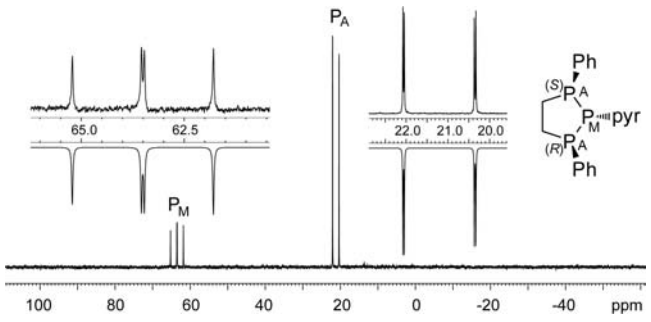

Figure 7. $^{31}P\{^{1}H\}$ NMR spectrum of **24** (CD_2Cl_2, 300 K; insets show experimental (upward) and fitted spectra (downward)); A_2M spin system ($\delta(P_A)$ = 21.2 ppm, $\delta(P_M)$ = 63.5 ppm, $^{1}J(P_AP_M)$ = −277.5 Hz).

A_2M spin system ($\delta(P_A)$ = 21.2 ppm, $\delta(P_M)$ = 63.5 ppm, $^{1}J(P_AP_M)$ = −277.5 Hz, CD_2Cl_2, 300 K) are observed and indicate the all-trans arrangement of the aryl substituents. The chemical shift of P_A is comparable to that of the corresponding nuclei in **19** (P_X) and to those of corresponding resonances in related 1,2,3-triphosphacyclopentane derivatives.[32] The resonance corresponding to P_M in **24** is shifted to significantly lower field due to the electron-withdrawing effect of the pyrazolyl substituent.[23] The $^{1}J(P_AP_M)$ coupling constant (−277.5 Hz) is similar to that of **19**. By analogy with the discussion of the conformation of **19** in solution, a time-averaged ^{2}E conformation can also be assumed for *all-trans*-**24** (Figure 3, **C**). Furthermore, the $^{31}P\{^{1}H\}$ NMR spectrum of the supernatant solution displays resonances corresponding to *rac*- and *meso*-bis(phenylphosphanyl)ethane derivatives **25**^{c,m}, and minor amounts of polyphosphanes **26**^{I,II} and **27**^{c,m} are observed (vide infra).

It was found that the mixture of diastereomers of octaphosphane **27**^{c,m} can be selectively prepared from **18**^{c,m} and **14** in CH_3CN if a ratio of 6:4 is employed. Compounds **27**^{c,m} were obtained as a colorless precipitate in decent yield (54%, Scheme 10). It is important to note that only *meso*-**18**^{m}

Scheme 10. Formation of Diasteriomeric Polyphosphanes *rac*-27^{c} (only the (*R*,*R*) enantiomer is shown) and *meso*-(*R*,*S*)-27^{m} from the Reaction of 18^{c,m} and 14 in a 6:4 Ratio[a]

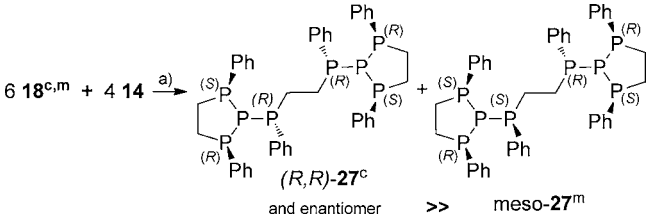

[a](a) −12 **17**, CH_3CN, over night, RT, 54%; an approximate 1:1 mixture of **18**^{c} and **18**^{m} was employed.

can react with **14** according to reaction path type I (Scheme 7) to form the favored and exclusively observed (vide infra) *all-trans*-1,2,3-triphosphacyclopentane moieties in **27**^{c,m}. Thus, the formation of a mixture of diastereomers **27**^{c,m} results from the incorporation of either the chiral *rac*-1,2-bis(phosphanyl)ethane moiety in *rac*-**27**^{c} or the *meso*-*R*,*S*-moiety in *meso*-**27**^{m} as the central bis(phosphanyl)ethane fragment. As the major amount of employed *meso*-**18**^{m} is consumed in the formation of the five-membered ring moieties, the probability of incorporation of the *rac*-bis(phosphanyl)ethane moiety, i.e., the formation of *rac*-**27**^{c} is higher than the formation of *meso*-**27**^{m}.

Accordingly, the $^{31}P\{^{1}H\}$ NMR spectrum of the isolated mixture of diastereomers **27**^{c,m} dissolved in C_6D_6 reveals two sets of signals corresponding to *rac*-**27**^{c} and *meso*-**27**^{m}. The intensity of the resonances corresponding to *rac*-**27**^{c} is significantly higher than that of the resonances corresponding to *meso*-**27**^{m} if the NMR sample is measured immediately after preparation (Figure 8, bottom, resonances corresponding to *rac*-**27**^{c} are shown in blue, those of *meso*-**27**^{m} are shown in red for the high field resonance). Within 14 h, isomerization occurs

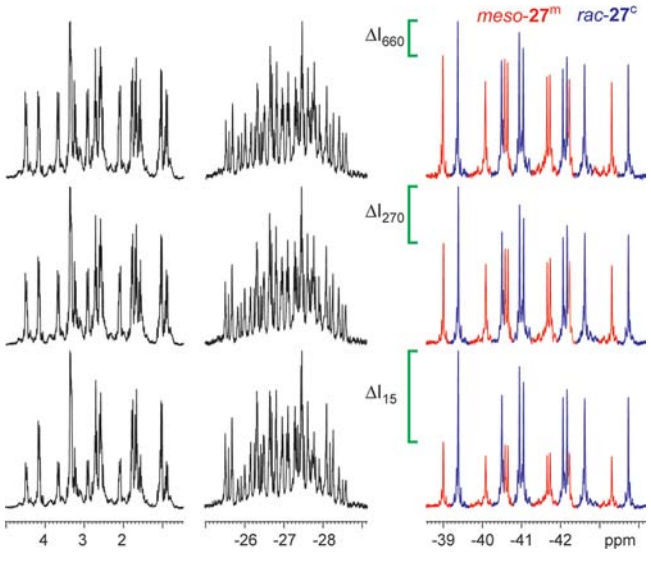

Figure 8. $^{31}P\{^{1}H\}$ NMR spectra of the mixture of diastereomers **27**^{c} (marked in blue for the high-field resonance, P_A) and **27**^{m} (marked in red for the high-field resonance, P_A) in C_6D_6; recording of the spectra commenced 15 (bottom), 270 (middle) and 660 (top) minutes after dissolution (512 scans each, PD = 2 s, 300 K).

dx.doi.org/10.1021/ja305406x | J. Am. Chem. Soc. 2012, 134, 15443−15456

in benzene solution to give an approximate 1:1 mixture of the diastereomers **27**^{c,m} (Figure 8). ΔI (green) indicates the approximate difference in the intensities of the resonances corresponding to the two distinct diastereomers). Significant decomposition of **27**^{c,m} in solution is observed after several days only. The observed isomerization is much faster in CH_2Cl_2 solution, giving the equilibrated mixture of diastereomers in less than 30 min. From such a sample, the $^{31}P\{^1H\}$ NMR parameters of **27**^{c,m} were derived by iterative fitting[33] of the experimental $^{31}P\{^1H\}$ NMR spectrum (Table 2). The

Table 2. $^{31}P\{^1H\}$ NMR Spectroscopic Parameters of the Diastereomers *rac*-27^c and *meso*-27^m Obtained from Iterative Fitting

		rac-**27**^{c}	meso-**27**^{m}
δ [ppm]	A	−41.5	−41.0
	M	−26.4	−26.9
	X	2.6	2.6
	Y	3.4	3.2
J [Hz][a,d]	$^1J(P_AP_M) = {}^1J(P_{A'}P_{M'})$	−178	−128
	$^1J(P_AP_X) = {}^1J(P_{A'}P_{X'})$	−269	−266
	$^1J(P_AP_Y) = {}^1J(P_{A'}P_{Y'})$	−254	−255
	$^2J(P_MP_X) = {}^2J(P_{M'}P_{X'})$	108	114
	$^2J(P_MP_Y) = {}^2J(P_{M'}P_{Y'})$	135	135
	$^2J(P_XP_Y) = {}^2J(P_{X'}P_{Y'})$	6	5
	$^3J(P_MP_{M'})$	−26	−28
	$^4J(P_AP_{M'}) = {}^4J(P_{A'}P_M)$	1[b]	1[b]
	$^5J(P_AP_{A'})$	0[c]	0[c]
	$^5J(P_MP_{X'}) = {}^5J(P_{M'}P_X)$	1[c]	1[c]
	$^5J(P_MP_{Y'}) = {}^5J(P_{M'}P_Y)$	2[c]	2[c]

[a]Decimal places of the coupling constants are not reported because of insufficient accuracy of the fit caused by the high complexity of the experimental $^{31}P\{^1H\}$ NMR spectrum and broad line widths at half height of the observed resonances. [b]Approximate value as the line width at half height is larger than the observed coupling constant. [c]Set value which was not iterated. [d]^6J and ^7J coupling constants were set to zero.

experimental and fitted spectra of the mixture of diastereomers as well as the deconvoluted spectra of *rac*-**27**^{c} and *meso*-**27**^{m} are presented in Figure 9. Both diastereomers are fitted as AA′MM′XX′YY′ spin systems. An approximate ratio of 48:52 (*rac*-**27**^{c}:*meso*-**27**^{m}) was deduced from the iterative fit of the concentration. The resonances corresponding to the P_A and P_M nuclei in both diastereomers ($\delta(P_A)$ = −41.5 ppm, $\delta(P_M)$ = −26.4 ppm (*rac*-**27**^{c}); $\delta(P_A)$ = −41.0 ppm, $\delta(P_M)$ = −26.9 ppm (*meso*-**27**^{m})) are in the expected range for the corresponding P atoms of isotetraphosphane fragments (vide supra). Similar to hexaphosphane **19**, the resonances corresponding to P_X and P_Y are observed at lowest field ($\delta(P_X)$ = 2.6 ppm, $\delta(P_Y)$ = 3.2 ppm (*rac*-**27**^{c}); $\delta(P_X)$ = 2.6 ppm, $\delta(P_Y)$ = 3.4 ppm (*meso*-**27**^{m})) in the typical region for P atoms incorporated in 1,2,3-triphosphacyclopentane rings.[28,32] The observation of three chemically unequal P atoms within each five-membered ring moiety indicates hindered rotation around the P_A−P_M bond. By analogy with the above discussion of **19**, a twist or a cis−trans conformation of the five-membered rings in solution can be excluded. The definite assignment of P_X and P_Y is not possible.

The magnitudes of the $^1J(P_AP_X)$ and $^1J(P_AP_Y)$ coupling constants ($^1J(P_AP_X)$ = −269 Hz, $^1J(P_AP_Y)$ = −254 Hz (*rac*-**27**^{c}); $^1J(P_AP_X)$ = −266 Hz, $^1J(P_AP_Y)$ = −255 Hz (*meso*-**27**^{m})) are comparable to those of the aforementioned 1,2,3-

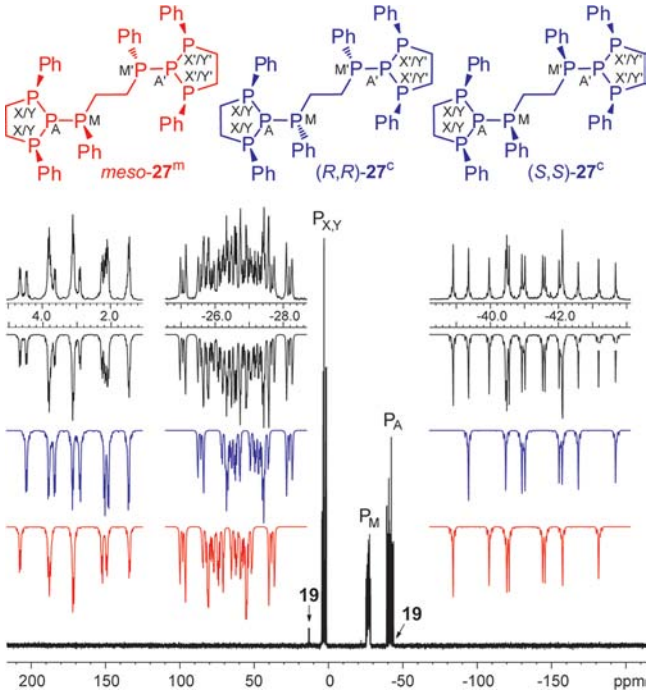

Figure 9. $^{31}P\{^1H\}$ NMR spectrum of **27**^{c,m} (CD_2Cl_2, 300 K; insets show experimental (upward) and fitted spectra of the mixture of diastereomers (black downward) and deconvoluted spectra of *rac*-**27**^{c} (blue, downward) and *meso*-**27**^{m} (red, downward); very small amounts of **19** indicate slow decomposition in solution.

triphosphacyclopentane derivatives (compare, for example, 1,2,3-triphenyl-1,2,3-triphosphacyclopentane $^1J(P_AP_B)$ = 273 Hz).[32] Coupling constants of similar size as the $^3J(P_MP_{M'})$ coupling constant in **27**^{c,m} are observed for other 1,2-bis(phosphanyl)ethane derivatives (e.g., 1-dimethylphosphino-2-diisopropylethane: $^3J(PP)$ = 25.2 Hz, C_6H_6).[37] The observed $^2J(P_MP_X)$ and $^2J(P_MP_Y)$ coupling constants are remarkably large ($^2J(P_MP_X)$ = 108 Hz, $^2J(P_{M'}P_{X'})$ = 135 Hz (*rac*-**27**^{c}); $^2J(P_MP_X)$ = 114 Hz, $^2J(P_{M'}P_{X'})$ = 135 Hz (*meso*-**27**^{m})). $^2J(PP)$ coupling constants in related isotetraphosphane moieties are generally smaller than 20 Hz (e.g., $(Me(Me_3Si)P)_2PP(SiMe_3)_2$: $^2J(PP)$ = 5.1 Hz).[38] By analogy with the discussion of the large $^3J(P_MP_{M'})$ coupling constant in **21** (vide supra), this is attributed to short distances between the lone pairs on P_M and $P_{X/Y}$ in **27**^{c,m}. This is in line with the proposed antiperiplanar arrangement with respect to the P_A−P_M bond which is exemplarily illustrated by the Newman projections along the P_A−P_M bonds of (*S*,*S*)-**27**^{c} depicted in Figure 10.[4] Similarly, large $^2J(PP)$ coupling constants due to close distances between the lone pairs of electrons on the involved P atoms were reported for polyphosphanes **29** ($^2J(PP)$ = 283.2 Hz)[39]

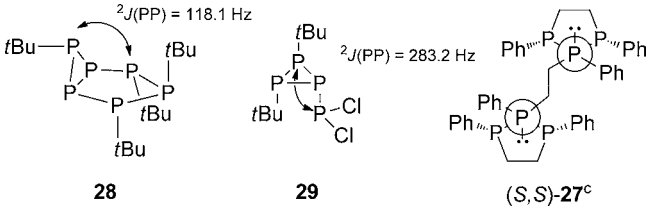

Figure 10. Examples of polyphosphanes featuring comparably large $^2J(PP)$ coupling constants and proposed conformation of (*S*,*S*)-**27**^{c}.

dx.doi.org/10.1021/ja305406x | J. Am. Chem. Soc. 2012, 134, 15443−15456

and **28** (^2J(PP) = 118.1 Hz[40]) as depicted in Figure 10. ^2J(PP) coupling constants within *all-trans*-1,2,3-triphosphacyclopentane fragments are rarely reported but seem to be much smaller or not observable[36] (e.g., 1,2,3-triethyl-1,2,3-triphospha-4-methylcyclopentane ^2J(PP) = 2.2 Hz).[28]

During our investigation, we succeeded in crystallizing *meso*-**27^{m}** from a very dilute CH_3CN solution of the diasteriomeric mixture of **27^{c,m}** (see Experimental Section for details). The obtained molecular structure is shown in Figure 11. The

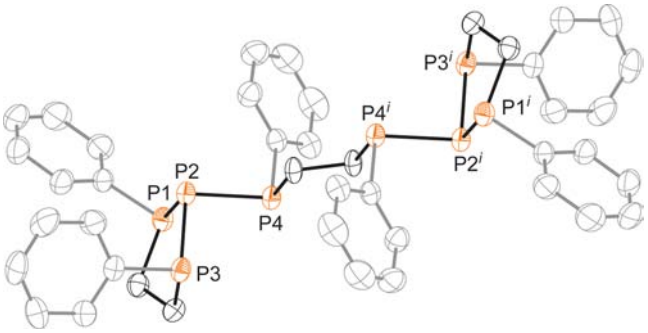

Figure 11. Molecular structure of *meso*-**27^{m}** (hydrogen atoms are omitted for clarity, and thermal ellipsoids are displayed at 50% probability); selected bond lengths [Å] and angles [deg]: P1−P2 2.224(1), P2−P3 2.194(1), P2−P4 2.218(1); P3−P2−P4 95.08(5), P3−P2−P1 97.97(5), P4−P2−P1 95.92(5); i = −*x*, −*y*, −*z*.

inversion symmetrical molecular structure of *meso*-**27^{m}** confirms the all-trans conformation of the triphosphacyclopentane moieties which was already deduced from spectroscopic observations in solution. The observed bond lengths and angles in this fragment are in agreement with the corresponding parameters in previously published, related triphosphacyclopentane derivatives.[41] Furthermore, an antiperiplanar conformation with respect to the P2−P4 bond is observed in the solid state which is similar to that proposed as the dominant conformation in solution.

While octaphosphanes **27^{c,m}** are formed from the reaction of **18^{c,m}** and **14** in a 1:0.66 ratio hexaphosphane **19** is obtained from reaction mixtures containing a 1:0.8 ratio of **18^{c,m}**:**14**. Therefore, it was of interest, if the diasteriomeric mixture of **27^{c,m}** would react with **14** to yield hexaphosphane **19**. It was found that the formation of **19** proceeds via three equilibrium reactions **I**−**III** (Scheme 11) involving the intermediates **24** and **26^{I,II}**. In the first step, **14** and **27^{c,m}** form triphosphacyclopentane **24** which subsequently reacts with a further equivalent of **27^{c,m}** in the second equilibrium reaction to form **19** and **26^{I,II}**. The latter reacts with **24** to form a second equivalent of **19** and **25^{c,m}**. All of these reactions represent P−N/P−P bond metathesis reactions according to Scheme 4. These conclusions are based on NMR spectroscopic investigations of mixtures of **27^{c,m}** and **14** in various ratios and are discussed in detail in the following paragraphs.

Figure 12A shows the $^{31}P\{^1H\}$ NMR spectrum of the reaction mixture of **27^{c,m}** and **14** in a 5:2 ratio in CH_2Cl_2 solution after a reaction time of 15 h. Resonances corresponding to **19** (vide supra) and **25^{c,m}** are observed. The latter was spectroscopically characterized. Removal of all volatiles from the reaction mixture in vacuo, stirring of the residue in CH_3CN, and storage at −35 °C gave a colorless suspension which was filtered. The obtained filtrate contained a mixture of diastereomers **25^{c,m}** (approximately 61%), **26^{I,II}**

Scheme 11. Formation of Hexaphosphane 19 via Three Equilibrium Reactions I−III Starting from 27^{c,m} and 14[a]

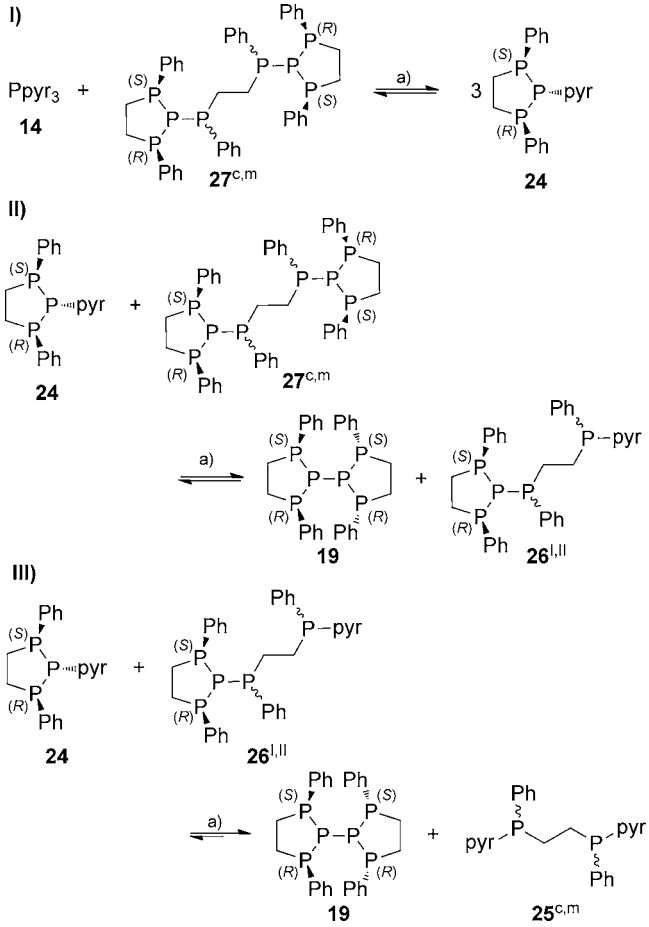

[a](a) CH_2Cl_2, RT, 15 h.

(approximately 38%), and **24** (<1% according to ^{31}P NMR spectroscopy). Further purification via recrystallization from common solvents, sublimation, or column chromatography under argon was not successful. However, multinuclear NMR spectroscopic investigations of the filtrate allowed for the identification of all resonances expected for **26^{I,II}** and **25^{c,m}** in the ^1H, $^{13}C\{^1H\}$, and $^{31}P\{^1H\}$ NMR spectra.

Next to the resonances of **24** and **25^{c,m}** four complex resonances are observed (Figure 12A). Of these, the resonance at lowest field can be clearly assigned to P_X of **19**. Close inspection of the remaining complex resonances revealed that these are composed of several overlapping signals. The group of signals at high field is composed of the resonances of five chemically unequal P nuclei. Figure 12 (enlargement B) shows the high field group of resonances (black) overlaid with the experimental spectra of **19** (red) and **27^{c,m}** (green). By comparison, the resonances of **19** and **27^{c,m}** can thus be assigned. Additionally, peaks corresponding to diastereomeric pentaphosphanes **26^{I,II}** are observed in this group of overlapping resonances. Similar analyses of the two remaining complex groups of resonances (Figure 12, C, D) reveal that each is composed of resonances corresponding to **27^{c,m}** (green) and **26^{I,II}**. A fourth resonance corresponding to **26^{I,II}** is found to overlap with the resonances of **25^{c,m}**. Each of the resonances of **26^{I,II}** displays a first-order dddd splitting which only in the case of the resonance at lowest field is not entirely resolved due

dx.doi.org/10.1021/ja305406x | J. Am. Chem. Soc. 2012, 134, 15443−15456

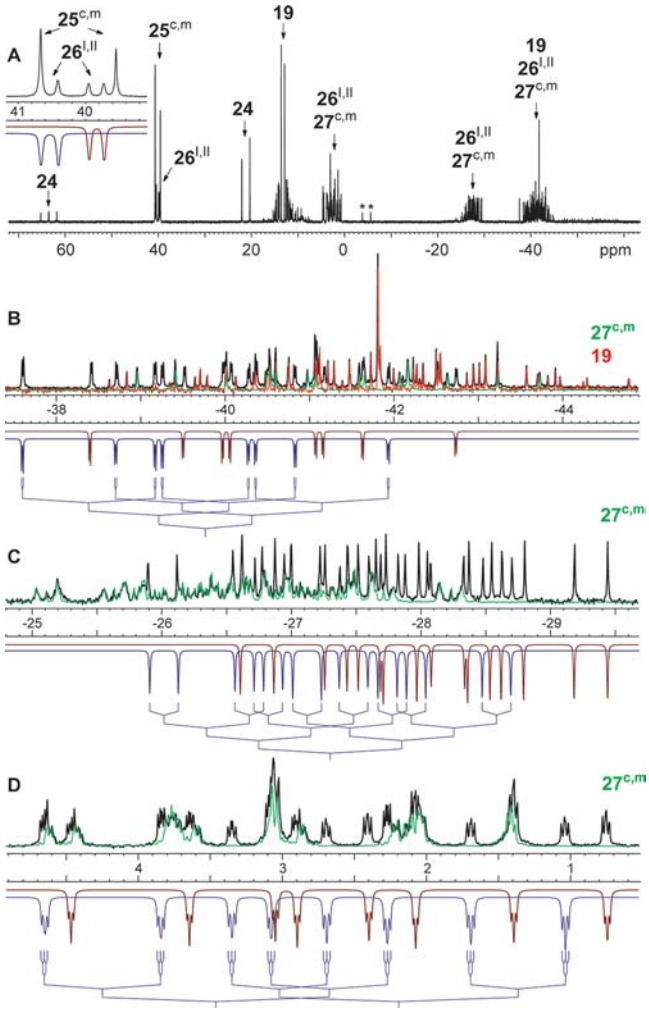

Figure 12. $^{31}P\{^1H\}$ NMR spectrum of the reaction mixture of **18**^{c,m} and **14** in a 5:2 ratio in CH_2Cl_2 solution after a reaction time of 15 h (A, CH_2Cl_2, C_6D_6 capillary, 300 K); inset and enlargements B–D show the experimental spectrum (upward, black) overlaid with the experimental spectra of pure **19** (upward, red, CD_2Cl_2, 300 K) and **27**^{c,m} (upward, green, CD_2Cl_2, 300 K) where applicable and the simulated spectra of the diastereomers of **26**^{I,II} (brown and blue, downward).

to increased line widths. Thus, the coupling constants were directly read from the experimental spectrum and used to simulate the $^{31}P\{^1H\}$ NMR spectra of **26**^{I,II}. The obtained simulated spectra of the two diastereomers are depicted in brown and blue in Figure 12 (A (inset), B–D, downward). The splitting pattern is exemplarily depicted for one diastereomer. The derived $^{31}P\{^1H\}$ NMR spectroscopic parameters of **26**^{I,II} which were used for the simulation are listed in Table 3.

The chemical shifts of the resonances corresponding to the P_A, P_M, P_X and P_Y nuclei of **26**^{I,II} and the observed coupling constants are very similar to the corresponding parameters of **27**^{c,m}. Therefore, it is very likely that pentaphosphanes **26**^{I,II} are structurally related to the isotetraphosphane moiety in **27**^{c,m}. Atoms P_Z display chemical shifts which are very similar to those of **25**^{c,m}. Thus, atoms P_Z can be assumed to bear a phenyl and a pyrazolyl substituent. The observed, prominent doublet splittings of these two resonances ($^3J(P_MP_Z)$ = −35.8 Hz (diastereomer 1), $^3J(P_MP_Z)$ = −42.0 Hz (diastereomer 2)) are comparable to the $^3J(P_MP_{M'})$ coupling constants in **27**^{c,m}

Table 3. $^{31}P\{^1H\}$ NMR Spectroscopic Parameters Derived from the Experimental Spectrum and used for the Simulation of the Spectra of 26^{I,II}

		diastereomer 1	diastereomer 2
δ [ppm]	A	−40.5	−39.7
	M	−27.4	−28.1
	X	2.2	1.9
	Y	3.4	3.3
	Z	39.8	40.5
J [Hz]	$^1J(P_AP_M)$	−179	−179
	$^1J(P_AP_X)$	−269	−269
	$^1J(P_AP_Y)$	−255	−255
	$^2J(P_MP_X)$	107	106
	$^2J(P_MP_Y)$	131	134
	$^2J(P_XP_Y)$	5	3
	$^3J(P_MP_z)$	−36	−42
	$^4J(P_AP_Z)$	3	4
	$^5J(P_XP_Z)$	3	4
	$^5J(P_YP_Z)$	3	3

($^3J(P_MP_{M'})$ = −26 Hz (*rac*-**27**^{c}), $^3J(P_MP_{M'})$ = −28 Hz (*meso*-**27**^{m})). Consequently, pentaphosphanes **26**^{I,II} are proposed to display the configuration depicted in Figure 13 (top). Given the

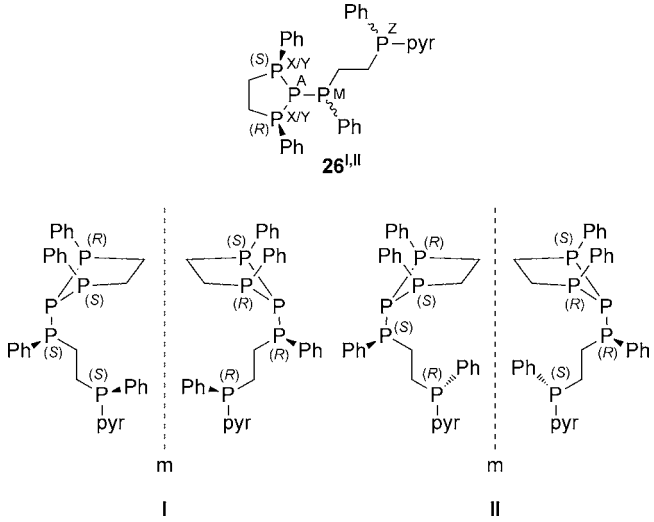

Figure 13. Configuration of pentaphosphanes **26**^{I,II} (top) and observed pair of diastereomers (**I**, **II**) comprising a pair of enantiomers each.

all-trans configuration of the five-membered ring (vide supra), two diastereomers (**I**, **II**) each comprising a pair of enantiomers are possible (Figure 13) and are observed in the $^{31}P\{^1H\}$ NMR spectrum. The unambiguous assignment of the resonances to the corresponding diastereomers is not possible.

The above reaction was carried out in a 5:2 ratio of **27**^{c,m}:**14**. Employing a 1:1 ratio instead, the $^{31}P\{^1H\}$ NMR spectrum presented in Figure 14 (green) is obtained from the reaction mixture after a reaction time of 15 h. The $^{31}P\{^1H\}$ NMR spectrum of the 5:2 reaction is also depicted in Figure 14 (red) for comparison. While minor amounts of starting material **14** are still present in the 1:1 reaction mixture, the increased amount of **14** apparently leads to the increased formation of **19** as indicated by the comparably higher intensities of the resonances of **19**. In contrast, significantly less intense

dx.doi.org/10.1021/ja305406x | J. Am. Chem. Soc. 2012, 134, 15443–15456

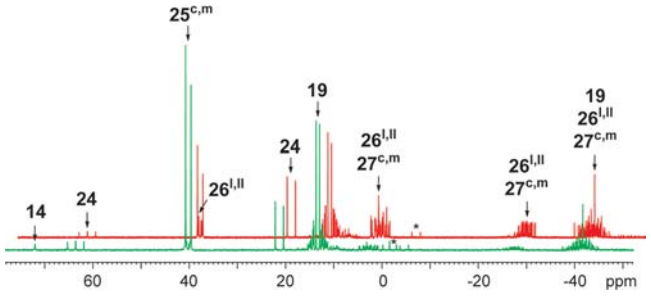

Figure 14. $^{31}P\{^{1}H\}$ NMR spectra of the reaction mixtures of $27^{c,m}$ and **14** in a 1:1 (green) and 5:2 (red) ratio in CH_2Cl_2 solution after reaction times of 15 h (C_6D_6 capillary, 300 K); * impurities.

resonances are observed for $27^{c,m}$ and $26^{I,II}$ in the spectrum of the 1:1 reaction compared to that of the reaction employing a 5:2 ratio. Overall, it is therefore concluded that the formation of **19** from $27^{c,m}$ and **14** proceeds via the intermediates $26^{I,II}$ and **24** as already depicted in Scheme 11. The addition of excess **14** shifts the equilibrium in favor of the formation of **19**. This detailed understanding of the reaction of $27^{c,m}$ with **14** allows for the formulation of a reaction equation for the formation of **19** from **14** and $18^{c,m}$ (Scheme 12).

Scheme 12. Reaction Equation for the Formation of 19 from $18^{c,m}$ and 14[a]

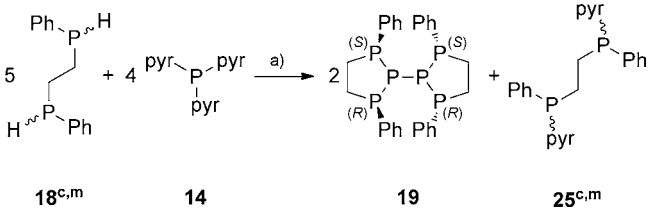

[a](a) −10 **17**, CH_3CN, RT, 20 h, 58%; an approximate 1:1 mixture of 18^{c} and 18^{m} was employed (according to ^{31}P NMR spectroscopy), but isomerization of the chiral P atoms occurs (vide supra).

Hexaphosphane **19** is formed in a unique combination of P−P bond formation via protolysis (type I, Scheme 7) and P−N/P−P bond metathesis reactions involving intermediates **24**, $26^{I,II}$, and $27^{c,m}$ from a 5:4 mixture of $18^{c,m}$:**14**. Employing a slight excess of **14** increases the isolated yield of **19** (58%) as a consequence of the shifting of the involved equilibrium reactions as described above.

CONCLUSION

In summary, an efficient one-pot synthesis of hexaphosphane **19** featuring a 2,2′-bi(1,2,3-triphosphacyclopentane) moiety was found. This compound represents the first isolable and fully characterized hexaphosphane comprising this type of branched polyphosphane motif. The stability of hexaphosphane **19** was demonstrated by the preparation of the unprecedented, dinuclear iron−carbonyl complex **21** which features hexaphosphane **19** as a bridging ligand. Detailed NMR spectroscopic investigations yielded an in-depth understanding of the mechanism of the formation of **19**. Unique ethylene-bridged bis-isotetraphosphanes $27^{c,m}$ were identified as intermediates, isolated and fully characterized.

Most importantly, this study demonstrates the applicability of P−N/P−P bond metathesis in the preparation of complex polyphosphanes (type II, Scheme 13). P−P bond formation of

Scheme 13. P−N/P−P Metathesis as a Powerful Strategy in the Synthesis of Complex Polyphosphanes

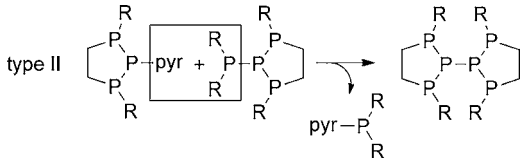

type II constitutes a reductive coupling of P atoms originating from **14** and is thus distinctly different from P−P bond formation of type I (Scheme 7). This constitutes a novel synthetic approach toward P−P bond formation starting from easily accessible pyrazolylphosphanes.

EXPERIMENTAL SECTION

All manipulations were performed in a Glovebox MB Unilab or using Schlenk techniques under an atmosphere of purified argon (Westfalen AG). Dry, oxygen-free solvents (CH_2Cl_2, CH_3CN (distilled from CaH_2, respectively), Et_2O, C_6H_6 (distilled from Na/benzophenone respectively), *n*-hexane (distilled from Na)) were employed. Deuterated benzene (C_6D_6) was purchased from Sigma-Aldrich and distilled from Na. Anhydrous deuterated acetonitrile (CD_3CN) and dichloromethane (CD_2Cl_2) were purchased from Sigma-Aldrich. All distilled and deuterated solvents were stored either over molecular sieves (4 Å; CH_2Cl_2, CH_3CN, C_6D_6, CD_2Cl_2, CD_3CN) or potassium mirror (*n*-hexane, Et_2O, C_6H_6). $Fe_2(CO)_9$ was purchased from Sigma-Aldrich. Tris(3,5-dimethyl-1-pyrazolyl)phosphane[22] and 1,2-bis-(phenylphosphanyl)ethane[24] were prepared according to literature procedures. All glassware was oven-dried at 160 °C prior to use. NMR spectra were measured on a Bruker AVANCE III (^{1}H (400.03 MHz), ^{13}C (100.59 MHz), ^{31}P (161.94 MHz)), at 300 K. All carbon-13 NMR spectra were exclusively recorded with broad band proton decoupling. Reported numbers of atoms in the ^{13}C spectra were indirectly deduced from the cross-peaks in 2D correlation experiments (HMBC, HSQC). Chemical shifts were referenced to δ_{TMS} = 0.00 ppm (^{1}H, ^{13}C) and $\delta_{H_3PO_4(85\%)}$ = 0.00 ppm (^{31}P, externally). Chemical shifts (δ) are reported in ppm. Coupling constants (J) are reported in hertz. Absolute values are reported, except for coupling constants derived by means of line shape iteration (vide infra). Assignments of individual resonances were performed using 2D techniques (HMBC, HSQC, HH−COSY, PP-COSY) where necessary. For compounds which give rise to a higher order spin-system in the $^{31}P\{^{1}H\}$ NMR spectrum, the resolution-enhanced $^{31}P\{^{1}H\}$ spectrum was transferred to the software gNMR, version 5.0.[33] The full line shape iteration procedure of gNMR was applied to obtain the best match of the fitted to the experimental spectrum. $^{1}J(^{31}P^{31}P)$ coupling constants were set to negative values,[42] and all other signs of the coupling constants were obtained accordingly. The designation of the spin system was performed by convention. The furthest downfield resonance is denoted by the latest letter in the alphabet, and the furthest upfield by the earliest letter. Melting points were recorded on an electrothermal melting point apparatus (Barnstead Electrothermal IA9100) in sealed capillaries under argon atmosphere and are uncorrected. Infrared (IR) and Raman spectra were recorded at ambient temperature using a Bruker Vertex 70 instrument equipped with a RAM II module (Nd:YAG laser, 1064 nm). The Raman intensities are reported in percent relative to the most intense peak and are given in parentheses. An ATR unit (diamond) was used for recording IR spectra. The intensities are reported relative to the most intense peak and are given in parentheses using the following abbreviations: vw = very weak, w = weak, m = medium, s = strong, vs = very strong, sh = shoulder. Elemental analyses were performed on a Vario EL III CHNS elemental analyzer at the IAAC, University of Münster, Germany.

X-ray Data Collection and Reduction. Suitable single crystals of **19** and **21** were obtained by slow diffusion of *n*-hexane into a solution of **19** in CH_2Cl_2 or by slow evaporation of a solution of **21** in toluene

dx.doi.org/10.1021/ja305406x | J. Am. Chem. Soc. 2012, 134, 15443−15456

at −30 °C. Single crystals of **27**^{m} were obtained from the NMR sample of the supernatant of the 5:2 reaction mixture of **27**^{c,m} and **14** in CD_3CN at room temperature. The crystals were coated with Paratone-N oil, mounted using a glass fiber-pin, and frozen in the cold nitrogen stream of the goniometer. X-ray diffraction data of compounds **19** and **21** were collected at 153(2) K on a Bruker AXS APEX CCD diffractometer equipped with a rotation anode K using graphite-monochromated Mo Kα radiation (λ = 0.71073 Å) and of **27**^{m} on Bruker Quazar CCD diffractometer equipped with a microfocus sealed tube using montel mirror-monochromated Mo Kα radiation (λ = 0.71073 Å). Diffraction data were collected over the full sphere, and the frames were integrated using the Bruker SMART[43] software package employing the narrow frame algorithm. Data were corrected for absorption effects using the SADABS routine (empirical multiscan method). For further crystal and data collection details, see Table 4.

Structure Solution and Refinement. Atomic scattering factors for non-hydrogen elements were taken from the literature tabulations. Structure solutions were found by using direct methods as implemented in the SHELXS-97 package[44] and were refined with SHELXL-97[45] against F^2, initially using isotropic and later anisotropic thermal parameters for all non-hydrogen atoms. Positions of hydrogen atoms were calculated and allowed to ride on the carbon atom to which they are bonded, assuming C−H bond length of 0.95 Å. H-atom temperature factors were set at 1.20 times the isotropic temperature factor of the C atom to which they are bonded. The H-atom contributions were calculated but not refined. Neither magnitude nor positions of the remaining peaks in the final difference Fourier map are of any chemical significance.

Table 4. Crystallographic Data and Details of the Structure Refinements of Compounds 19, 21, and 27^{m}

	19	**21**	**27**^{m}
formula	$C_{28}H_{28}P_6$	$C_{36}H_{28}Fe_2O_8P_6$	$C_{42}H_{42}P_8$
M_r [g mol^{-1}]	550.32	886.10	794.52
color, habit	colorless plate	yellow plate	colorless plate
crystal system	triclinic	monoclinic	monoclinic
space group	$P\bar{1}$	$C2/c$	$P2_1/c$
a [Å]	7.8833(9)	14.8647(5)	13.140(2)
b [Å]	9.520(1)	13.8772(5)	15.312(2)
c [Å]	9.840(1)	19.5756(7)	10.269(1)
α [deg]	96.954(2)	90	90
β [deg]	102.101(1)	110.079(1)	94.958(4)
γ [deg]	106.323(1)	90	90
V [Å^3]	680.1(1)	3792.6(2)	2058.4(4)
Z	1	4	2
T [K]	153(1)	153(1)	153(1)
crystal size [mm]	0.12 × 0.05 × 0.04	0.07 × 0.07 × 0.01	0.14 × 0.08 × 0.03
ρ_c [g cm^{-3}]	1.344	1.552	1.282
F(000)	286	1800	828
$\lambda_{Mo\ K\alpha}$ [Å]	0.71073	0.71073	0.71073
θ_{min} [deg], θ_{max} [deg]	2.16, 27.88	2.07, 27.87	1.56, 27.87
index range	$10 \geq h \geq -10$	$19 \geq h \geq -19$	$15 \geq h \geq -17$
	$12 \geq k \geq -11$	$18 \geq k \geq -18$	$20 \geq k \geq -13$
	$12 \geq l \geq -12$	$25 \geq l \geq -25$	$12 \geq l \geq -23$
μ [mm^{-1}]	0.412	1.069	0.368
absorption correction	SADABS	SADABS	SADABS
reflections collected	6398	19042	14406
reflections unique	3192	4532	4864
R_{int}	0.0155	0.0237	0.0496
reflections obsd [$F > 3\sigma(F)$]	2907	3936	3097
residual density [e Å^{-3}]	0.400 −0.194	0.359 −0.188	0.441 −0.277
parameters	154	235	226
GOOF	1.054	1.025	1.019
R_1 [$I > 2\sigma(I)$]	0.0278	0.0243	5.65
wR_2 (all data)	0.0750	0.0608	13.98
CCDC	883610	883611	883612

Preparation of 1,1′,3,3′-Tetraphenyl-2,2′-bi(1,2,3-triphospholane) (19). A solution of 1,2-bis(phenylphosphino)ethane

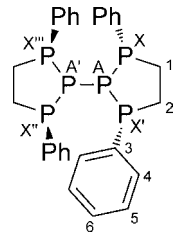

(**18**^{c,m}) (0.739 g, 3.00 mmol, 1.00 equiv, 1:1 mixture of the chiral (**18**^{c}) and meso (**18**^{m}) isomers) in CH_3CN (8 mL) was slowly added to a solution of tris(3,5-dimethyl-1-pyrazolyl)phosphane (0.739 g, 3.00 mmol, 1.00 equiv) in CH_3CN (12 mL). The initially colorless solution turned into a pale yellow suspension shortly after addition was completed. The mixture was stirred at ambient temperature for 24 h. The obtained colorless precipitate was filtered off and washed with CH_3CN (4 × 5 mL), and all volatiles were removed in vacuo. Single crystals suitable for X-ray single crystal structure determination were obtained via slow diffusion of *n*-hexane into a solution of **19** in CH_2Cl_2 at ambient temperature. The filtrate was further processed for the isolation of **24** (vide infra). Yield: 0.381 g (58%); mp: 197−199 °C; Raman (100 mW, [cm^{-1}]): 3085(7), 3047(71), 2943(12), 2923(26), 2897(60), 1583(81), 1569(8), 1431(6), 1409(11), 1156(15), 1096(26), 1027(48), 997(100), 687(6), 636(16), 618(12), 495(27), 469(23), 427(39), 402(8), 325(6), 299(8), 263(11), 240(18), 201(25), 169(39), 120(8), 104(35); IR (ATR, [cm^{-1}]): 3647(vw), 2942(vw), 2889(w), 1581(w), 1567(vw), 1474(w), 1428(w), 1402(w), 1325(vw), 1301(vw), 1256(vw), 1224(vw), 1175(vw), 1151(w), 1112(vw), 1064(w), 1024(w), 996(w), 967(vw), 870(w), 782(w), 740(vs), 694(s), 644(w), 634(w), 498(m), 482(w), 452(w); ^{1}H NMR (CD_2Cl_2, 300 K, [ppm]): δ = 7.40 (8H, m, C4-H), 7.23 (12H, m, C5-H, C6-H), 2.82 (8H, m, C1-H, C2-H); ^{13}C{^{1}H} NMR (CD_2Cl_2, 300 K, [ppm]): δ = 138.4 (4C, C3), 132.4 (8C, C4), 128.8 (8C, C5), 128.3 (4C, C6), 32.9 (4C, C1, C2); ^{31}P{^{1}H} NMR (CD_2Cl_2, 300 K, [ppm]): AA′XX′X″X‴ spin system: $\delta(P_A)$ = −41.8 (2P), $\delta(P_X)$ = 13.2 (4P); $^1J(P_AP_{A'})$ = −137.0 Hz, $^1J(P_AP_X)$ = $^1J(P_AP_{X'})$ = $^1J(P_{A'}P_{X''})$ = $^1J(P_{A'}P_{X'''})$ = −258.5 Hz, $^2J(P_AP_{X''})$ = $^2J(P_AP_{X'''})$ = $^2J(P_{A'}P_X)$ = $^2J(P_{A'}P_{X'})$ = 142.5 Hz, $^2J(P_XP_{X'})$ = $^2J(P_{X''}P_{X'''})$ = 1.9 Hz, $^3J(P_XP_{X''})$ = $^3J(P_{X'}P_{X''})$ = 31.7 Hz, $^3J(P_XP_{X''})$ = $^3J(P_{X'}P_{X''})$ = 49.5 Hz; elemental analysis: calcd for $C_{28}H_{28}P_6$: C: 61.1, H: 5.1, found: C: 59.6, H: 4.9; MS-ESI-EM: 551.0692 (MH^+), calcd for $C_{28}H_{29}P_6$: 551.0873.

Preparation of 1,1′-(1,1′,3,3′-Tetraphenyl-2,2′-bi(1,2,3-triphospholane))bis(iron(0)tetracarbonyl) (21). THF (80 mL)

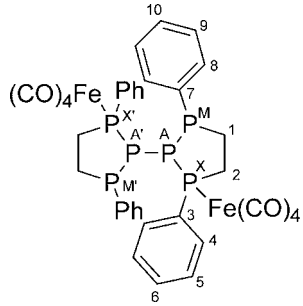

was added to a mixture of **19** (0.37 g, 0.66 mmol, 1 equiv) and $Fe_2(CO)_9$ (0.485 g, 1.33 mmol, 2 equiv) in the dark. The mixture was

dx.doi.org/10.1021/ja305406x | J. Am. Chem. Soc. 2012, 134, 15443−15456

stirred for 72 h. Slow dissolution of the orange crystals of $Fe_2(CO)_9$ was observed. All volatiles were removed from the mixture in vacuo, and the resulting solid was dissolved in toluene (80 mL). Slow removal of toluene in vacuo and storage at −18 °C yielded **21** as pale orange crystals. Yield: 0.161 g (28%); mp: decomp at T > 120 °C; Raman (10 mW, [cm^{-1}]): 3059(49), 2942(10), 2916(52), 2055(28), 1986(74), 1937(87), 1922(10), 1595(47), 1516(9), 1189(6), 1158(9), 1102(15), 1028(31), 1003(100), 666(9), 641(7), 618(14), 480(11), 466(21), 439(72), 406(9), 330(22), 217(7); IR (ATR, [cm^{-1}]): 3058(vw), 2905(vw), 2046(s), 1978(w), 1913(vs, br, sh), 1582(vw), 1481(vw), 1433(w), 1415(vw), 1400(vw), 1302(vw), 1230(vw), 1186(vw), 1118(vw), 1089(w), 999(w), 876(w), 784(w), 742(m), 691(m), 666(w), 608(vs), 514(m); ^{1}H NMR (THF-d_8 , 300 K, [ppm]): δ = 7.61 (4H, m, C4-H), 7.25 (6H, m, C5-H, C6-H), 7.14 (4H, m, C8-H), 7.08−6.98 (6H, m, C9-H, C10-H), 3.61 (2H, m, $\nu_{1/2}$ = 26.4 Hz, C2-H), 3.16 (2H, m, $\nu_{1/2}$ = 42.2 Hz, C1-H), 2.98 (2H, pseudo quint, C2-H), 2.63 (2H, m, $\nu_{1/2}$ = 27.6 Hz, C1-H); ^{1}H{^{31}P} NMR (THF-d_8 , 300 K, [ppm]): δ = 7.61 (4H, m, C4-H), 7.25 (6H, m, C5-H, C6-H), 7.14 (4H, m, C8-H), 7.08−6.98 (6H, m, C9-H, C10-H) 3.61 (2H, ddd, $^2J_{C2\text{-}H,C2\text{-}H}$ = 15.0 Hz, $^3J^{gauche}_{C2\text{-}H,C1\text{-}H}$ = 5.5 Hz, $^3J^{anti}_{C2\text{-}H,C1\text{-}H}$ = 5.2 Hz, C2-H), 3.16 (2H, ddd, $^2J_{C1\text{-}H,C1\text{-}H}$ = 13.7 Hz, $^3J^{gauche}_{C2\text{-}H,C1\text{-}H}$ = 5.5 Hz, $^3J^{anti}_{C2\text{-}H,C1\text{-}H}$ = 6.3 Hz, C1-H), 2.98 (2H, ddd, $^2J_{C2\text{-}H,C2\text{-}H}$ = 15.0 Hz, $^3J^{gauche}_{C2\text{-}H,C1\text{-}H}$ = 9.3 Hz, $^3J^{anti}_{C2\text{-}H,C1\text{-}H}$ = 6.3 Hz, C2-H), 2.63 (2H, ddd, $^2J_{C1\text{-}H,C1\text{-}H}$ = 13.7 Hz, $^3J^{gauche}_{C2\text{-}H,C1\text{-}H}$ = 9.3 Hz, $^3J^{anti}_{C2\text{-}H,C1\text{-}H}$ = 5.2 Hz, C1-H); ^{13}C{^{1}H} NMR (THF-d_8, 300 K, [ppm]): δ = 214.5 (8C, pseudo tt, CO), 137.8 (2C, m, C3), 137.1 (2C, m, C7), 132.1 (4C, pseudo sept, C8), 130.9 (6C, m, C4, C6), 129.6 (4C, m, C5), 128.9 (4C, pseudo t, C9), 128.8 (2C, s, C10), 40.1 (2C, pseudo t, C2), 31.6 (2C, pseudo t, C1); ^{31}P{^{1}H} NMR (THF-d_8, 300 K, [ppm]): AA′MM′XX′ spin system: $\delta(P_A)$ = −47.4 (2P), $\delta(P_M)$ = 15.3 (2P), $\delta(P_X)$ = 93.0 (2P); $^1J(P_AP_{A'})$ = −317.5 Hz, $^1J(P_AP_M)$ = $^1J(P_{A'}P_{M'})$ = −314.0 Hz, $^1J(P_AP_X)$ = $^1J(P_{A'}P_{X'})$ = −276.7 Hz, $^2J(P_AP_{M'})$ = $^2J(P_{A'}P_M)$ = −2.0 Hz, $^2J(P_AP_{X'})$ = $^2J(P_{A'}P_X)$ = 103.1 Hz, $^2J(P_MP_X)$ = $^2J(P_{M'}P_{X'})$ = 1.1 Hz, $^3J(P_MP_{M'})$ = 163.8 Hz, $^3J(P_MP_{X'})$ = $^3J(P_{M'}P_X)$ = 5.3 Hz, $^3J(P_XP_{X'})$ = 51.0 Hz; elemental analysis: calcd for $C_{36}H_{28}Fe_2O_8P_6$: C: 48.8, H: 3.2, found: C: 49.4, H: 3.2.

Isolation and Spectroscopic Characterization of 1-(1,3-Diphenyl-1,2,3-triphospholan-2-yl)-3,5-dimethylpyrazole (24).

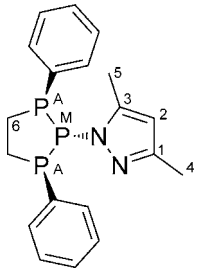

From the filtrate prepared according to the synthetic procedure for **19**, triphosphane **24** was isolated by column chromatography under argon employing Al_2O_3 (dried at 380 °C for 72 h) as the stationary phase in a column of 2.5 cm in diameter which was filled to a height of 15 cm. Et_2O was used as the eluent and 20 fractions of 5 mL were collected. **24** was isolated from fractions 11−13 (yield: 8 mg) and was characterized by means of ^{1}H and ^{31}P{^{1}H} NMR spectroscopy. It decomposed in solution during the measurement of the ^{13}C{^{1}H} NMR spectrum which prevented the assignment of the resonances. ^{1}H NMR (CD_2Cl_2 , 300 K, [ppm]): δ = 7.26−7.18 (10 H, m, Ph), 5.85 (1H, d, ^4J(HP) = 2.6 Hz, C2-H), 3.20 (2H, m, C6-H), 2.85 (2H, m, C6-H), 2.45 (3H, s, C5-H), 2.19 (3H, s, C4-H); ^{31}P{^{1}H} NMR (CD_2Cl_2, 300 K, [ppm]): A_2M spin system: $\delta(P_A)$ = 21.2 (2P), $\delta(P_M)$ = 63.5 (1P); $^1J(P_AP_M)$ = −277.5 Hz.

Preparation of a Mixture of Diastereomers 1-((1*R*)-((1*R*,3*S*)-1,3-Diphenyl-1,2,3-triphospholan-2-yl)(phenyl)phosphino)-2-((1*S*)-((1*R*,3*S*)-1,3-diphenyl-1,2,3-triphospholan-2-yl)(phenyl)-phosphino)ethane (27^m) and *rac*-1,2-Bis(((1*R*,3*S*)-1,3-diphenyl-1,2,3-triphospholan-2-yl)(phenyl)phosphanyl)ethane (27^c). A solution of 1,2-bis(phenylphosphino)ethane (**18**^{c,m}) (0.19 g, 0.75 mmol, 1.5 equiv, 1:1 mixture of the chiral (**18**^{c}) and meso (**18**^{m}) isomers) in CH_3CN (2 mL) was slowly added to a solution of tris(3,5-dimethyl-1-pyrazolyl)phosphane (0.16 g, 0.50 mmol, 1.0 equiv) in CH_3CN (3 mL). A colorless oil formed during the addition which gradually turned into a colorless solid. The mixture was stirred overnight. The resulting colorless suspension was filtered. The obtained solid was stirred in CH_3CN (5 × 8 mL) for 20 min, filtered off, respectively, and dried in vacuo. Obtained **27**^{c,m} is a mixture of the diastereomers **27**^{m} and **27**^{c} in a ratio of approximately 48(**27**^{c}):52(**27**^{m}). [Remark: The phenyl substituents on a single triphosphacyclopentane moiety are chemically inequivalent. As the resonances in the ^{1}H and ^{13}C spectra corresponding to these substituents are not separated, both substituents are marked uniformly as *A*.] Yield: 0.108 g (54%); mp: 161−163 °C; Raman (50 mW, [cm^{-1}]): 3048(81), 2922(11), 2899(38), 1584(50), 1408(11), 1247(6), 1156(13), 1093(14), 1027(27), 1000(100), 738(17), 690(9), 640(9), 617(8), 510(12), 464(11), 426(18), 238(10), 202(12), 138(14); IR (ATR, [cm^{-1}]): 3046(vw), 2896(vw), 1583(vw), 1478(w), 1431(m), 1406(w), 1303(vw), 1224(vw), 1183(vw), 1155(w), 1080(vw), 1064(w), 1025(w), 999(w), 870(w), 787(m), 739(s), 722(w), 692(vs), 666(w), 647(m), 508(w), 499(s), 482(m), 465(w), 453(w); ^{1}H NMR (CD_2Cl_2 , 300 K, [ppm]): δ = 7.70 (8H, m, $C_{ortho}(B)$-H), 7.37 (4H, m, $C_{para}(B)$-H), 7.36 (8H, m, $C_{meta}(B)$-H), 7.29 (8H, m, $C_{ortho}(A)$-H), 7.21−7.11 (32H, $C_{meta}(A)$-H, $C_{ortho}(A)$-H, $C_{para}(A)$-H), 2.63−2.17 (24H, m, CH_2); ^{13}C{^{1}H} NMR (CD_2Cl_2, 300 K, [ppm]): δ = 138.1 (8C, m, $C_{ipso}(A)$), 136.2 (4C, m, $C_{ipso}(B)$), 134.5 (8C, m, $C_{ortho}(B)$), 132.5 (8C, pseudo-ddd, $C_{ortho}(A)$), 132.2 (8C, pseudo-ddd, $C_{ortho}(A)$), 129.9 (2C, pseudo-t, $C_{para}(B)$), 129.8 (2C, pseudo-t, $C_{para}(B)$), 128.8−128.5 (24C, m, $C_{meta}(A,B)$), 128.3(4C, pseudo-t, $C_{para}(A)$), 128.1 (4C, pseudo-t, $C_{para}(A)$), 32.7 (4C, pseudo-dd, $CH_2(C)$), 32.2 (4C, pseudo-d, $CH_2(C)$), 25.1 (4C, s(broad), $\nu_{1/2}$ = 44 Hz, $CH_2(D)$); ^{31}P{^{1}H} NMR (CD_2Cl_2, 300 K, [ppm]): *rac*-**27**^{c}: AA′MM′XX′YY′ spin system: $\delta(P_A)$ = −41.5 (2P), $\delta(P_M)$ = −26.4 (2P), $\delta(P_X)$ = 2.6 (2P), $\delta(P_Y)$ = 3.4 (2P); $^1J(P_AP_M)$ = $^1J(P_{A'}P_{M'})$ = −178 Hz, $^1J(P_AP_X)$ = $^1J(P_{A'}P_{X'})$ = −269 Hz, $^1J(P_AP_Y)$ = $^1J(P_{A'}P_{Y'})$ = −254 Hz, $^2J(P_MP_X)$ = $^2J(P_{M'}P_{X'})$ = 108 Hz, $^2J(P_MP_Y)$ = $^2J(P_{M'}P_{Y'})$ = 135 Hz, $^2J(P_XP_Y)$ = $^2J(P_{X'}P_{Y'})$ = 6 Hz, $^3J(P_MP_{M'})$ = −26 Hz, $^4J(P_AP_{M'})$ = $^4J(P_{A'}P_M)$ = 1 Hz, $^5J(P_AP_{A'})$ = 0 Hz, $^5J(P_MP_{X'})$ = $^5J(P_{M'}P_X)$ = 1 Hz, $^5J(P_MP_{Y'})$ = $^5J(P_{M'}P_Y)$ = 2 Hz, ^6J and ^7J coupling constants were not observed; *meso*-**27**^{m}: AA′MM′XX′YY′ spin system:

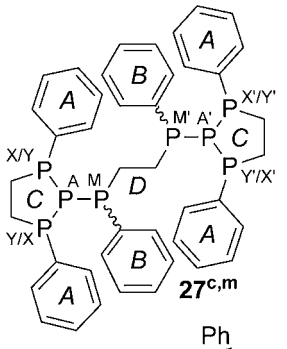

27^{c,m}

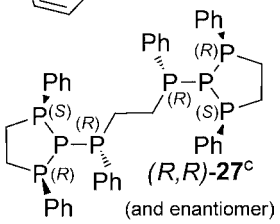

(*R*,*R*)-**27**^{c} (and enantiomer)

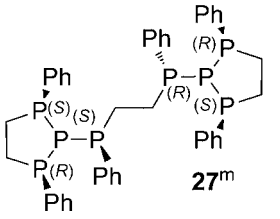

27^m

dx.doi.org/10.1021/ja305406x | J. Am. Chem. Soc. 2012, 134, 15443−15456

$\delta(P_A) = -41.0$ (2P), $\delta(P_M) = -26.9$ (2P), $\delta(P_X) = 2.6$ (2P), $\delta(P_Y) = 3.2$ (2P); $^1J(P_AP_M) = {}^1J(P_{A'}P_{M'}) = -173$ Hz, $^1J(P_AP_X) = {}^1J(P_{A'}P_{X'}) = -266$ Hz, $^1J(P_AP_Y) = {}^1J(P_{A'}P_{Y'}) = -255$ Hz, $^2J(P_MP_X) = {}^2J(P_{M'}P_{X'}) = 114$ Hz, $^2J(P_MP_Y) = {}^2J(P_{M'}P_{Y'}) = 135$ Hz, $^2J(P_XP_Y) = {}^2J(P_{X'}P_{Y'}) = 5$ Hz, $^3J(P_MP_{M'}) = -28$ Hz, $^4J(P_AP_{M'}) = {}^4J(P_{A'}P_M) = 1$ Hz, $^5J(P_AP_{A'}) = 0$ Hz, $^5J(P_MP_{X'}) = {}^5J(P_{M'}P_X) = 1$ Hz, $^5J(P_MP_{Y'}) = {}^5J(P_{M'}P_Y) = 2$ Hz, ^6J and ^7J coupling constants were not observed; elemental analysis: calcd for $C_{42}H_{42}P_8$: C: 63.5, H: 5.2, found: C: 63.4, H: 5.3; MS-ESI-EM: 795.1271 (MH^+), calcd for $C_{42}H_{43}P_8$: 795.7266; 519.0849 (M, −1,3-diphenyl-1,2,3-triphospholide), calcd for $C_{28}H_{28}P_5$: 519.0879.

Reactions of $\mathbf{27^{c,m}}$ *with* **14**. *1. Reaction in a 5:2 Ratio. Spectroscopic Characterization of* $\mathbf{25^{c,m}}$ *and* $\mathbf{26^{I,II}}$. A solution of **14** (10.1 mg, 0.032 mmol, 2 equiv) in CH_2Cl_2 (0.5 mL) was added to a solution of $\mathbf{27^{c,m}}$ (63.6 mg, 0.080 mmol, 5 equiv) in CH_2Cl_2 (0.5 mL). The resulting pale yellow solution was stirred for 15 h. ^1H, ^{31}P, and $^{31}P\{^1H\}$ NMR spectra of the mixture were measured (C_6D_6 capillary, 300 K). The resonances observed in the $^{31}P\{^1H\}$ NMR spectrum, which is depicted in Figures 12 and 14, are listed below. The spin systems of $\mathbf{26^{I,II}}$ were analyzed in detail (Figure 12), and the derived parameters are also listed below. All volatiles were removed in vacuo from the remaining reaction mixture resulting in the formation of a semicrystalline, colorless residue which was suspended in CH_3CN (1 mL) and filtered. The filtrate was stored at −35 °C for 15 h, resulting in the formation of small amounts of a colorless precipitate which were filtered off. All volatiles were removed from the filtrate in vacuo, yielding a colorless solid which was found to contain approximately 1:1 mixtures of the diastereomers of $\mathbf{25^{c,m}}$ as the major component (approximately 64%) and the diastereomers of $\mathbf{26^{I,II}}$ (approximately 33%) as well as minor amounts of unidentified byproduct. Further purification of $\mathbf{25^{c,m}}$ via crystallization, sublimation, or column chromatography was not successful. However, multinuclear NMR experiments (CD_3CN, 300 K) of the enriched sample of $\mathbf{25^{c,m}}$ allowed for the assignment of the resonances corresponding to $\mathbf{25^{c,m}}$ and $\mathbf{26^{I,II}}$ in the ^1H, $^{13}C\{^1H\}$, and $^{31}P\{^1H\}$ NMR spectra which are given below. Resonances observed in the $^{31}P\{^1H\}$ NMR spectrum of the reaction mixture: $^{31}P\{^1H\}$ NMR (CH_2Cl_2, C_6D_6 capillary, 300 K, [ppm]): $\delta = 63.6$ (m, M-part of the A_2M spin system of **24**), 40.7 (s, $\mathbf{25^{c/m}}$), 40.6 (dddd, Z-part of the AMXYZ spin system of **26**, diastereomer 2), 39.9 (dddd, Z-part of the AMXYZ spin system of **26**, diastereomer 1), 39.6 (s, $\mathbf{25^{c/m}}$), 21.3 (m, A-part of the A_2M spin system of **24**), 13.3 (m, X-part of the AA′XX′X″X‴ spin system of **19**), 4.9−0.8 (m, X- and Y-parts of the AA′MM′XX′YY′ spin systems of $\mathbf{27^{c,m}}$ and X- and Y-parts of the AMXYZ spin systems of **26**, diastereomers 1 and 2), −4.6 (m, unassigned), −25.7−(−29.4) (m, M-parts of the AA′MM′XX′YY′ spin systems of $\mathbf{27^{c,m}}$ and the AMXYZ spin systems of **26**, diastereomers 1 and 2), −37.4−(−45.0) (m, A-parts of the AA′XX′X″X‴ spin system of **19**, the AA′MM′XX′YY′ spin systems of $\mathbf{27^{c,m}}$ and the AMXYZ spin systems of **26**, diastereomers 1 and 2).$^{31}P\{^1H\}$ NMR Parameters of $\mathbf{26^{I,II}}$ in the Reaction Mixture Diastereomer 1: $^{31}P\{^1H\}$ NMR (CH_2Cl_2, C_6D_6 capillary, 300 K); AMXYZ spin system: $\delta(P_A) = -40.5$ ppm (1P), $\delta(P_M) = -27.4$ ppm (1P), $\delta(P_X) = 2.2$ ppm (1P), $\delta(P_Y) = 3.4$ ppm (1P), $\delta(P_Z) = 39.8$ ppm (1P); $^1J(P_AP_M) = -179.0$ Hz, $^1J(P_AP_X) = -269.0$ Hz, $^1J(P_AP_Y) = -255.0$ Hz, $^2J(P_MP_X) = 107.0$ Hz, $^2J(P_MP_Y) = 131.0$ Hz, $^2J(P_XP_Y) = 4.5$ Hz, $^3J(P_MP_Z) = -35.8$ Hz, $^4J(P_AP_Z) = 3.0$ Hz, $^5J(P_XP_Z) = 3.4$ Hz, $^5J(P_YP_Z) = 3.0$ Hz. Diastereomer 2: $^{31}P\{^1H\}$ NMR (CH_2Cl_2, C_6D_6 capillary, 300 K); AMXYZ spin system: $\delta(P_A) = -39.7$ ppm (1P), $\delta(P_M) = -28.1$ ppm (1P), $\delta(P_X) = 1.9$ ppm (1P), $\delta(P_Y) = 3.3$ ppm (1P), $\delta(P_Z) = 40.5$ ppm (1P); $^1J(P_AP_M) = -179.0$ Hz, $^1J(P_AP_X) = -269.0$ Hz, $^1J(P_AP_Y) = -255.0$ Hz, $^2J(P_MP_X) = 106.0$ Hz, $^2J(P_MP_Y) = 134.0$ Hz, $^2J(P_XP_Y) = 3.0$ Hz, $^3J(P_MP_Z) = -42.0$ Hz, $^4J(P_AP_Z) = 3.5$ Hz, $^5J(P_XP_Z) = 3.0$ Hz, $^5J(P_YP_Z) = 3.0$ Hz.Resonances Observed in the $^{31}P\{^1H\}$ NMR Spectrum of the Enriched Sample of $\mathbf{25^{c,m}}$ ^1H NMR (CD_3CN, 300 K, [ppm]): δ = 7.71−7.60 (m, C13-H ($\mathbf{26^{I,II}}$)), 7.50−7.07 (m, C_{aryl}-H ($\mathbf{25^{c,m}}$), C_{aryl}-H ($\mathbf{26^{I,II}}$)), 5.89 (s, C2-H, ($\mathbf{25^{c,m}}$), C2-H ($\mathbf{26^{I,II}}$)), 2.67−2.47 (m, C10-H, ($\mathbf{25^{c,m}}$), C10-H, C11-H ($\mathbf{26^{I,II}}$)), 2.62−2.27 (m, C20-H, C21-H, ($\mathbf{26^{I,II}}$), 2.40−2.33 (m, C5-H, ($\mathbf{25^{c,m}}$), C5-H ($\mathbf{26^{I,II}}$)), 2.20−2.01 (m, C10-H, ($\mathbf{25^{c,m}}$), C10-H, C11-H ($\mathbf{26^{I,II}}$)), 2.18−2.10 ($\mathbf{25^{c,m}}$), 2.15−2.12 (m, C4-H, ($\mathbf{25^{c,m}}$), C4-H ($\mathbf{26^{I,II}}$)); $^{13}C\{^1H\}$ NMR (CD_3CN, 300 K, [ppm]): δ = 153.5−153.4 (m, C1 ($\mathbf{25^{c,m}}$), C1 ($\mathbf{26^{I,II}}$)), 149.4−148.9 (m, C3 ($\mathbf{25^{c,m}}$), C1 ($\mathbf{26^{I,II}}$)), 139.2−139.0 (m, C6 ($\mathbf{25^{c,m}}$), C6, C12, C16 ($\mathbf{26^{I,II}}$)), 134.9 (m, C13 ($\mathbf{26^{I,II}}$)), 132.7 (m, C17 ($\mathbf{26^{I,II}}$)), 132.4−132.0 (m, C7 ($\mathbf{26^{c,m}}$), C7 ($\mathbf{26^{I,II}}$)), 130.9−130.6 (m, C9 ($\mathbf{25^{c,m}}$), C9, C15 ($\mathbf{26^{I,II}}$)), 129.5 (m, C8 ($\mathbf{25^{c,m}}$), C8, C14, C18 ($\mathbf{26^{I,II}}$)), 129.0 (s, C19 ($\mathbf{26^{I}}$ or $\mathbf{26^{II}}$)), 128.9 (s, C19 ($\mathbf{26^{I}}$ or $\mathbf{26^{II}}$)), 107.7 (m, C2 ($\mathbf{25^{c,m}}$), C2 ($\mathbf{26^{I,II}}$)), 32.7 (m, C20 or C21 ($\mathbf{26^{I,II}}$)), 32.4 (m, C20 or C21 ($\mathbf{26^{I,II}}$)), 25.6−25.5 (m, C10 ($\mathbf{25^{c,m}}$), C10, C11 ($\mathbf{26^{I,II}}$)), 14.1 (s, C4 ($\mathbf{25^{c,m}}$), C4 ($\mathbf{26^{I,II}}$)), 12.7−12.5 (m, C5 ($\mathbf{25^{c,m}}$), C5 ($\mathbf{26^{I,II}}$)); $^{31}P\{^1H\}$ NMR (CD_3CN, 300 K, [ppm]): δ = 40.3 (s, $\mathbf{26^{c/m}}$), 39.9 (m, Z-parts of the AMXYZ spin systems of $\mathbf{26^{I,II}}$), 39.9 (s, $\mathbf{25^{c/m}}$), 37.6 (m, unassigned), 4.6−1.3 (m, X- and Y-parts of the AMXYZ spin systems of $\mathbf{26^{I,II}}$), −26.0−(−29.9) (m, M-parts of the AMXYZ spin systems of $\mathbf{26^{I,II}}$), −37.3−(−42.2) (m, A-parts of the AMXYZ spin systems of $\mathbf{26^{I,II}}$).

2. Reaction in a 1:1 Ratio. A solution of **14** (6.4 mg, 0.02 mmol, 1 equiv) in CH_2Cl_2 (0.5 mL) was added to a solution of $\mathbf{27^{c,m}}$ (15.9 mg, 0.02 mmol, 1 equiv) in CH_2Cl_2 (0.5 mL). The resulting pale yellow solution was stirred for 15 h. ^1H, ^{31}P, and $^{31}P\{^1H\}$ NMR spectra were recorded (C_6D_6 capillary, 300 K). The following resonances were observed in the $^{31}P\{^1H\}$ NMR spectrum which is depicted in Figure 14. $^{31}P\{^1H\}$ NMR (CH_2Cl_2, C_6D_6 capillary, 300 K, [ppm]): δ = 72.0 (s, **14**), 63.6 (m, M-part of the A_2M spin system of **24**), 40.8 (s, $\mathbf{25^{c/m}}$), 40.6 (dddd, Z-part of the AMXYZ spin system of **26**, diastereomer 2), 39.9 (dddd, Z-part of the AMXYZ spin system of **26**, diastereomer 1), 39.6 (s, $\mathbf{25^{c/m}}$), 21.3 (m, A-part of the A_2M spin system of **24**), 13.3 (m, X-part of the AA′XX′X″X‴ spin system of **19**), 4.9−0.8 (m, X- and Y-parts of the AA′MM′XX′YY′ spin systems of $\mathbf{27^{c,m}}$ and X- and Y-parts of the AMXYZ spin systems of $\mathbf{26^{I,II}}$), −1.6 (m, unassigned), −4.6 (m, unassigned), −25.7−(−29.4) (m, M-parts of the AA′MM′XX′YY′ spin systems of $\mathbf{27^{c,m}}$ and the AMXYZ spin systems of $\mathbf{26^{I,II}}$), −37.4−(−45.0) (m, A-parts of the AA′XX′X″X‴ spin system of **19**, the AA′MM′XX′YY′ spin systems of $\mathbf{27^{c,m}}$ and the AMXYZ spin systems of $\mathbf{26^{I,II}}$).

■ ASSOCIATED CONTENT

Ⓢ Supporting Information

Crystallographic information files. This material is available free of charge via the Internet at http://pubs.acs.org.

■ AUTHOR INFORMATION

Corresponding Author

jweigand@uni-muenster.de

Notes

The authors declare no competing financial interest.

■ ACKNOWLEDGMENTS

We appreciate having been financially supported by the Fonds der Chemischen Industrie (fellowship to K.-O.F.), the DFG (WE 4621/2-1), the European COST network PhosSciNet (CM0802), and the ERC (SynPhos 307616). J.J.W. thanks Prof. F. Ekkehardt Hahn (WWU Muenster) for his support, and Prof. Robert Wolf (University of Regensburg) for helpful discussions.

■ REFERENCES

(1) Gomez-Ruiz, S.; Hey-Hawkins, E. *Coord. Chem. Rev.* **2011**, *255*, 1360.

(2) (a) Scheer, M.; Balazs, G.; Seitz, A. *Chem. Rev.* **2010**, *110*, 4236. (b) Giffin, N. A.; Masuda, J. D. *Coord. Chem. Rev.* **2011**, *255*, 1342.

(3) (a) Hönle, W.; von Schnering, H. G. *Z. Kristallogr.* **1980**, *153*, 339. von Schnering, H. G.; Hönle, W. Phosphides: Solid State Chemistry. In *Encyclopedia of Inorganic Chemistry*; King, R. B., Ed.; Wiley: Chichester, U.K., 1994; p 3106. (c) Pöttgen, R.; Hönle, W.; von Schnering, H. G. Phosphides: Solid State Chemistry. In *Encyclopedia of Inorganic Chemistry*, 2nd ed.; King, R. B., Ed.; Wiley: Chichester, U.K., 2005; Vol. *VIII*, p 4255, and reference therein.

(4) (a) Baudler, M. *Angew. Chem., Int. Ed. Engl.* **1982**, *21*, 492. (b) Baudler, M. *Angew. Chem., Int. Ed.* **1987**, *26*, 419. (c) Baudler, M.; Glinka, K. *Chem. Rev.* **1993**, *93*, 1623. (d) Baudler, M.; Glinka, K. *Chem. Rev.* **1994**, *94*, 1273.
(5) (a) Fritz, G. *Comments Inorg. Chem.* **1982**, *6*, 329. (b) Fritz, G. *Adv. Inorg. Chem.* **1987**, 171.
(6) Luo, Y. R. *Comprehensive Handbook of Chemical Bond Energies*; CRC Press: Boca Raton, 2007.
(7) (a) Haiduc, I. *The Chemistry of Inorganic Ring Systems*; Wiley-Interscience: London, 1970. (b) Kosolapoff, G. M.; Maier, L. *Organic Phosphorus Compounds*; Wiley-Interscience: New York, 1972.
(8) (a) Maier, L. *Helv. Chim. Acta* **1966**, *49*, 1119. (b) Niecke, E.; Rüger, R.; Krebs, B. *Angew. Chem., Int. Ed. Engl.* **1982**, *21*, 544. (c) Burg, A. B. *J. Am. Chem. Soc.* **1961**, *83*, 2226. (d) Jurkschat, K.; Mugge, C.; Tzschach, A.; Uhlig, W.; Zschunke, A. *Tetrahedron Lett.* **1982**, *23*, 1345. (e) Mazieres, M. R.; Rauzy, K.; Bellan, J.; Sanchez, M.; Pfister-Guillouzo, G.; Senio, A. *Phosphorus, Sulfur, Silicon* **1993**, *76*, 45.
(9) (a) Etkin, N.; Fermin, M. C.; Stephan, D. W. *J. Am. Chem. Soc.* **1997**, *119*, 2954. (b) Greenberg, S.; Stephan, D. W. *Chem. Soc. Rev.* **2008**, *37*, 1482. (c) Gómez-Ruiz, S.; Frank, R.; Gallego, B.; Zahn, S.; Kirchner, B.; Hey-Hawkins, E. *Eur. J. Inorg. Chem.* **2011**, 739.
(10) (a) Less, R. J.; Melen, R. L.; Naseri, V.; Wright, D. S. *Chem. Commun.* **2009**, 4929. (b) Beswick, M. A.; Choi, N.; Harmer, C. N.; Hopkins, A. D.; McPartlin, M.; Wright, D. S. *Science* **1998**, *281*, 1500.
(11) (a) Waterman, R. *Cur. Org. Chem.* **2008**, *12*, 1322. (b) Böhm, V. P. W.; Brookhart, M. *Angew. Chem., Int. Ed.* **2001**, *40*, 4694.
(12) Kovacs, I.; Krautscheid, H.; Matern, E.; Fritz, G. *Z. Anorg. Allg. Chem.* **1994**, 1369.
(13) (a) Fritz, G.; Mayer, B.; Matern, E. *Z. Anorg. Allg. Chem.* **1992**, *607*, 19. (b) Kovacs, I.; Fritz, G. *Z. Anorg. Allg. Chem.* **1994**, *620*, 1. (c) Fritz, G.; Goesmann, H.; Mayer, B. *Z. Anorg. Allg. Chem.* **1992**, *607*, 26. (d) Fritz, G.; Vaahs, T. *Z. Anorg. Allg. Chem.* **1987**, *552*, 18.
(14) Baudler, M.; Reuschenbach, G.; Hahn, J. *Z. Anorg. Allg. Chem.* **1981**, *482*, 27.
(15) Fritz, G.; Vaahs, T. *Z. Anorg. Allg. Chem.* **1987**, *553*, 85.
(16) Avens, L. R.; Cribbs, L. V.; Mills, J. L. *Inorg. Chem.* **1989**, *28*, 211.
(17) Cowley, A. H.; Dierdorf, D. S. *J. Am. Chem. Soc.* **1969**, *91*, 6609.
(18) Carey, F. A.; Sundberg, J. *Advanced Organic Chemistry, Part B: Reactions and Synthesis*, 5th ed.; Springer: New York, 2008.
(19) Avens, L. R.; Cribbs, L. V.; Mills, J. L. *Inorg. Chem.* **1989**, *28*, 205.
(20) (a) Weigand, J. J.; Feldmann, K.-O.; Echterhoff, A. K. C.; Ehlers, A. W.; Lammertsma, K. *Angew. Chem., Int. Ed.* **2010**, *49*, 6178. (b) Feldmann, K.-O.; Schulz, S.; Klotter, F.; Weigand, J. J. *ChemSusChem* **2011**, *4*, 1805.
(21) (a) Feldmann, K.-O.; Weigand, J. J. *Angew. Chem., Int. Ed.* **2012**, *51*, 6566. (b) Feldmann, K.-O.; Weigand, J. J. *Angew. Chem., Int. Ed.* **2012**, *51*, 7545.
(22) Fischer, S; Peterson, L. K.; Nixon, J. F. *Can. J. Chem.* **1974**, *52*, 3981.
(23) Feldmann, K.-O.; Fröhlich, R.; Weigand, J. J. *Chem. Commun.* **2012**, *48*, 4296.
(24) Issleib, K.; Weichmann, H. *Chem. Ber.* **1968**, *101*, 2197.
(25) Dyker, C. A.; Riegel, S. D.; Burford, N.; Lumsden, M. D.; Decken, A. *J. Am. Chem. Soc.* **2007**, *129*, 7464.
(26) Pople and Cremer ring puckering analysis: (a) Cremer, D.; Pople, J. A. *J. Am. Chem. Soc.* **1975**, *97*, 1354. (b) Spek, A. L. *J. Appl. Crystallogr.* **2003**, *36*, 7.
(27) von Schnering, H. G.; May, W. *Z. Naturforsch. B* **1978**, *33*, 698.
(28) Baudler, M.; Tolls, E.; Clef, E.; Koch, V; Kloth, B. *Z. Anorg. Allg. Chem.* **1979**, *456*, 5.
(29) Strauss, H. L. *Annu. Rev. Phys. Chem.* **1983**, *34*, 301.
(30) Albrand, J. P.; Robert, J. B. *Chem. Commun.* **1974**, 644.
(31) Scheer, M.; Gremler, S.; Herrmann, E.; Grünhagen, U.; Dargatz, M.; Kleinpeter, E. *Z. Anorg. Allg. Chem.* **1991**, *600*, 203.
(32) Baudler, M.; Vesper, J.; Sandmann, H. *Z. Naturforsch. B* **1972**, *27*, 1007.
(33) Budzelaar, P. H. M. *gNMR for Windows* (5.0.6.0). NMR Simulation Program, IvorySoft **2006**).
(34) (a) Gil, V. M. S.; von Philipsborn, W. *Magn. Reson. Chem.* **1989**, *27*, 409. (b) McFarlane, H. C. E.; McFarlane, W. *J. Chem. Soc., Chem. Commun.* **1975**, 582.
(35) Del Bene, J. E.; Elguero, J. *J. Phys. Chem. A* **2006**, *110*, 12543.
(36) Hitchcock, P. B.; Lappert, M. F.; Leung, W.-P.; Yin, P. *J. Chem. Soc., Dalton Trans.* **1995**, 3925.
(37) Brown, L. D.; Datta, S.; Kouba, J. K.; Smith, L. K.; Wreford, S. S. *Inorg. Chem.* **1978**, *17*, 729.
(38) Fritz, G.; Jarmer, M.; Matern, E. *Z. Anorg. Allg. Chem.* **1990**, *586*, 47.
(39) Baudler, M.; Makowka, B. *Z. Anorg. Allg. Chem.* **1985**, *528*, 7.
(40) Baudler, M.; Aktalay, Y.; Tebbe, K.-F.; Heinlein, T. *Angew. Chem., Int. Ed. Engl.* **1981**, *11*, 967.
(41) (a) von Schneering, H. G.; May, W. *Z. Naturforsch. B* **1978**, *33*, 698. (b) Kazul'kin, D. N.; Ryabov, A. N.; Izmer, V. V.; Churakov, A. V.; Beletskaya, I. P.; Burns, C. J.; Voskoboynikov, A. Z. *Organometallics* **2005**, *24*, 3024.
(42) (a) McFarlane, H. C. E.; McFarlane, W.; Nash, J. *Dalton Trans.* **1980**, 240. (b) Aime, S.; Harris, R. K.; McVicker, E. M.; Fild, M. *Dalton Trans.* **1976**, 2144. (c) Forgeron, M. A. M.; Gee, M.; Wasylishen, R. E. *J. Phys. Chem.* **2004**, *108*, 4895. (d) Del Bene, J. E.; Elguero, J.; Alkorta, I. *J. Phys. Chem.* **2004**, *108*, 3662.
(43) *SMART*; Bruker AXS, 2000 program package.
(44) Sheldrick, G. M. *Acta Crystallogr.* **1990**, *A46*, 467.
(45) Sheldrick, G. M. *SHELXL-97*; Universität Göttingen, 1997.